

Chris André Sylstad

---

## Testosterone and Skeletal Muscle Memory

The effects of testosterone on a C2C12 cell culture model of skeletal muscle memory

---

Master thesis in  
Department of Physical Performance  
Norwegian School of Sport Sciences, 2023

This page is intentionally not left blank

## Acknowledgements

Five years ago, on the other side of the planet sitting on a rock perched over the landscapes of the Australian bush, I decided to dedicate the next half decade of my life to learn as much as I possibly could while pursuing a degree within the field of human exercise, health, and performance. Today, as I write the final words of my master thesis, I look back on five incredibly productive years, filled with a ridiculous amount of reading, writing, talking, sparring, sacrifice, new friends, and most of all learning. I am deeply grateful to be allowed this incredible privilege and look forward to applying the teachings I have gathered to continue building a fulfilling life that will inspire others to pursue their values and dreams. The human mind and body is an incredibly beautiful piece of art, which this degree gave me the absolute pleasure of exploring for countless hours, and the skills and habits to continue to do so for the rest of my life.

To all my friends and family that have endured my ramblings and absence the past five years, I thank you! Your love, support, and belief in me are an essential part of my successes which I could not have managed without.

To my supervisor Prof. Adam Sharples, thank you for the generous opportunity to join your laboratory and learn from the best. Your guidance and feedback in the planning, design, and writing of this project was immensely helpful.

A special thank you to Dr. Daniel Turner, your patience and guiding hand in the gritty wet-work in the laboratory made this entire project possible. Your feedback, patience, and humour staved me from going crazy in the hardest of times and I am incredibly grateful for this.

As I conclude this chapter of my academic journey, I am reminded that as one door closes, many more await to be opened. I am excited to embark on new adventures, armed with the knowledge and experiences I have gained through this incredible journey. With gratitude and determination in my soul, I eagerly embrace the next chapter of my life.



*Chris André Sylstad, June 2023*

## Abstract

**Introduction:** Testosterone is vital for skeletal muscle (SkM) development and exhibits a dose-response relationship with muscle characteristics. However, the underlying molecular mechanisms are not fully understood. Recent studies on SkM memory, in the context of resistance training, have identified myonuclear permanence and epigenetic methylation as key mechanisms. Given similarities between testosterone and resistance training outcomes, it is plausible that testosterone may influence SkM memory, with implications for hormone replacement strategies, anti-doping regulations, age-related muscle decline, and our understanding of testosterone mechanisms. **Purpose:** To investigate the effects of repeated testosterone treatment on SkM memory using a C2C12 cell culture model. **Method:** C2C12 myoblast cells were subjected to six treatment conditions: Control, early, two late, and two repeated treatments (memory), receiving a supraphysiological testosterone dose at specific time-points after myotube differentiation. Morphological imaging, fixation for myonucleic counting, RNA for PCR analysis (Androgen receptor (AR), myosin heavy chains/MHC I, 2, 4, and 7 genes), and DNA for methylation analysis were collected. **Results:** Myotube numbers remained unchanged across conditions and time. Treated conditions showed a significant increase in myotube diameter and area compared to control. Memory conditions had a greater increase in diameter than single treated conditions. The repeated treatments with testosterone availability exhibited greater myotube area than all other conditions. Moreover, also exhibiting larger myobranches than nearly all other conditions. No significant differences in gene expression were observed for any condition. Memory conditions tended to deviate non-significantly from all other conditions. AR gene remained unchanged, but repeated treatment tended for reduced expression in memory conditions. Fast twitch MHC isoforms exhibited gradual increases, with less pronounced increase in repeated treatments. Slow twitch MyHC isoforms tended for increase expression on day 3 for early single treatment, plateauing by day 7 and 10, while memory conditions exhibited a decreasing trend. **Conclusion:** Testosterone augment C2C12 hypertrophy, with repeated treatment resulting in additional hypertrophy provided testosterone availability, with evidence of memory effects within myotube diameter and area. Single-dose testosterone minimally affected gene expression, while repeated treatment showed non-significant reduction in AR gene expression, slow twitch MyHC isoform, and less pronounced increases in fast twitch MyHC isoforms. These findings suggest saturation of ARs and a shift in cell priorities to non-traditional actions due to repeated testosterone treatment.

## Table of Contents

Acknowledgements .....	III
Abstract .....	IV
Part I – Introduction.....	1
1.0 Background .....	1
1.2 Thesis and Study Objective.....	3
Part II – Theory.....	3
2.0 Testosterone biosynthesis in vivo.....	3
2.0.1 Peripheral synthesis of androgens .....	4
2.1 Testosterone in skeletal muscle .....	4
2.2 Testosterone pathways .....	5
2.3 Testosterone effects on satellite- and mesenchymal stem cells .....	9
2.4 Overlapping signal transduction pathways between Testosterone and RT .....	10
2.2 Skeletal muscle memory .....	10
2.3 Epigenetics .....	12
2.3.1 Histone Modifications .....	12
2.3.2 Non-coding RNA .....	13
2.3.3 DNA Methylation.....	13
2.3.4 Epigenetic skeletal muscle memory .....	14
2.4 Evidence for SkM memory of previous testosterone use .....	15
2.5 Implications for sports, doping, transgender athletes, and the ageing population .....	16
Part III - Methodology .....	17
3.0 Cell culture as an in vitro model of skeletal muscle.....	17
3.0.1 C2C12 Skeletal muscle myoblasts .....	18
3.1 Methods .....	18
3.1.1 Study design .....	18
3.1.2 General Cell Culture .....	19
3.1.3 Cell Treatment .....	21
3.1.4 Morphological Analysis .....	23
3.1.5 RNA isolation and RT-QRT-PCR.....	24
3.2.0 Statistical analysis.....	26
Part IV – Results and Discussion .....	27
4.0 Results .....	27
4.0.1 Morphological analysis .....	27

4.1.0 Gene expression analysis .....	37
4.2.0 Discussion .....	46
4.2.1 Main findings.....	46
4.2.2 The effects of testosterone treatment on C2C12 morphology.....	47
4.2.3 The effects of testosterone treatment on C2C12 fold gene expression.....	50
4.2.4 C2C12 memory of previous testosterone treatment .....	52
4.2.5 Limitations of this thesis .....	53
4.3.0 Conclusions and future directions .....	55
V. List of figures .....	56
VI. References .....	57
Appendix A .....	74
Attestation of Authorship and the use of Artificial Intelligence .....	74

## Part I – Introduction

### 1.0 Background

Androgens are hormones regulating the differentiation, development, and maintenance of male characteristics in vertebrates through actions mostly mediated by binding to androgen-receptors (AR) leading to genomic actions (Basaria, 2013; Bennett et al., 2009; Hughes et al., 2016; Nussey & Whitehead, 2001). Of these, Testosterone and its metabolite, dihydrotestosterone, remains the predominant and most biologically vital androgens (Nussey & Whitehead, 2001). Interestingly, a strong dose-response-like relationship is observed between testosterone administration and skeletal muscle (SkM) mass and strength, including improved recovery after exercise (Bhasin et al., 1996, 2001, 2005; Forbes, 1985; Sinha-Hikim et al., 2002). AR-mediated gene transcription is also associated with more optimal body composition and physical function, cognition, bone health, and cardiometabolic health. More specifically acting upon cell proliferation, differentiation, apoptosis, metabolism, signalling cascades, gene transcription, and secretory activity. Establishing androgens as a fundamental pillar of tissue growth and homeostasis for both males and females (Basaria, 2013; Bennett et al., 2009; Corona et al., 2016; Nussey & Whitehead, 2001). Despite extensive studies, many of the molecular mechanisms behind testosterone-mediated effects on SkM remain elusive. Particularly, (i) the exact molecular pathways involved with mesenchymal pluripotent- (MSC) and SkM satellite- stem cell (SC) differentiation and lineage commitment (e.g., myogenic vs. adipogenic vs. pool-replenishment). (ii) Whether the increase in motor neuron number and size contribute to the anabolic effects of testosterone. (iii) The exact contribution of coactivators in AR-mediated genomic actions (Dubois et al., 2012; Herbst & Bhasin, 2004), and (iv) whether androgens alter the epigenetic [and/or myonucleic] landscape in a retentive fashion, akin to those observed by resistance exercise: training, detraining, and retraining models (TDR-model). Whereby retention of myonucleic and/or epigenetic modifications have been associated with SkM possessing a memory of previous and adequate anabolic stimuli (Bruusgaard et al., 2010; Egner et al., 2013; Seaborne et al., 2018; Sharples, Stewart, et al., 2016; Turner et al., 2019).

The past few centuries muscle memory was synonymous with today's "motor-learning", i.e., the central nervous system establishing neural pathways for specific movements allowing them to be performed at near automation. The notion of muscle memory as the ability to regain SkM mass

and strength after a period of de-training has anecdotally been referenced by bodybuilders, strongmen, and gym-goers for decades (Gundersen, 2016). Which has in later years gained scientific traction with two theories of action dominating the literature: (i) Myonuclear permanence, and (ii) epigenetic memory (Sharples, Stewart, et al., 2016; Snijders et al., 2020). The main tenet of the prior being that exercise-induced increases in myonuclei are retained during prolonged de-training as to facilitate an augmented re-training period (i.e., by having more ‘factories’ for protein synthesis per area of muscle fiber); (Snijders et al., 2020). Whereas for the latter, an epigenetic methylation pattern either up- or down-regulating expression of target genes is retained throughout the de-training period and enables augmented re-training through heightened transcriptional activity (Li et al., 2014; Riba et al., 2019; Sharples, Stewart, et al., 2016). Indeed, several genes [associated with ...] → extra cellular matrix and actin remodeling, mechano-transduction and TGF- $\beta$  signaling (Turner et al., 2019), are identified to have retentive methylation patterns in training, de-training, and re-training models (TDR-models); (Seaborne et al., 2018; Turner et al., 2019). Conversely, the myonucleic permanence mechanism has struggled to provide sufficient data to support its hypothesis in humans, mainly due to poor study design and methods, but show clear retentive mechanisms in rodents (Snijders et al., 2020).

It is not unlikely that testosterone influences muscle memory akin to resistance training (RT), considering its effects on myonuclei and gene transcription recapitulates several mechanisms observed by RT alone (Bennett et al., 2009; Braga et al., 2012; Yue Chen et al., 2005; Dubois et al., 2012; Egan & Zierath, 2013; Ferrando et al., 1998, 2002; Griggs et al., 1989; Haren et al., 2011; Herbst & Bhasin, 2004; Nelson et al., 2002). Moreover, crosstalk between RT and androgenic receptor mechanisms has been observed (Cardaci et al., 2020). Additionally, the AR modulates expression of several genes associated with skeletal muscle development and function (Wyce et al., 2010). The implications of a memory mechanisms of previous testosterone use could affect the current positions on hormone replacement strategies, doping-bans in sports, inclusion of trans-female athletes in traditionally cis-gender sports, provide with strategies to attenuate age or disease-related declines in muscle mass and strength, and expand our understanding of the mechanisms of epigenetic memory and testosterone.



## 1.2 Thesis and Study Objective

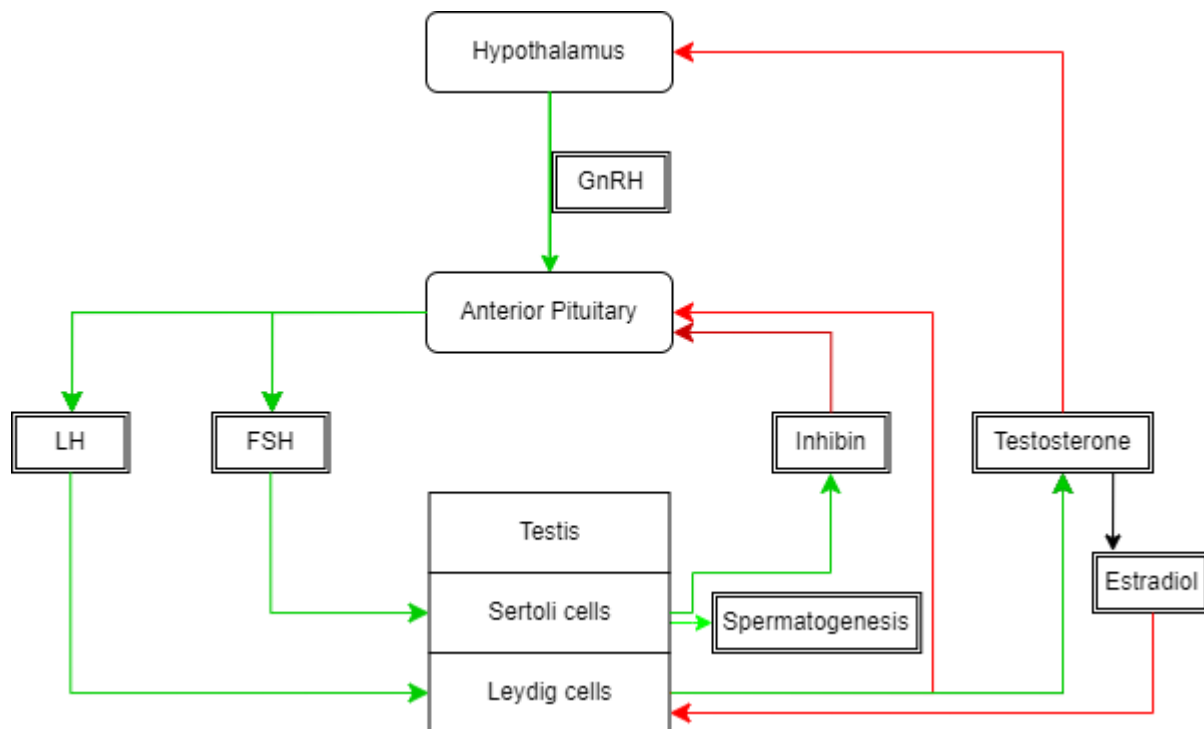
The objectives of this thesis are to investigate whether testosterone facilitates a memory response in SkM akin to that observed in TDR-models. There is scarcity in research investigating the potential memory mechanisms of previous testosterone use, with one single mouse model at its basis. Here the evidence points to a strong memory mechanism facilitated by myonuclear accretion and retention (Egner et al., 2013). This thesis will therefore add to this knowledge by investigating the effects of testosterone on (i) morphology, (iii) gene expression (iv) epigenetic methylation and (iv) myonuclear retention, in a C2C12 cell culture model of testosterone memory.

However, substantial delays in the experiment due to unforeseen circumstances resulted in only the morphological and gene expression analysis being completed on time (see limitations).

## Part II – Theory

### 2.0 Testosterone biosynthesis in vivo

Androgens are synthesised from cholesterol in the testes, the ovaries, and the adrenal glands, whereas testosterone is produced almost exclusively in the testes of males or secreted in smaller amounts from the adrenal cortex and ovaries in females (Miller & Auchus, 2011; Nussey & Whitehead, 2001). Testosterone synthesis is regulated by the hypothalamic-pituitary-gonadal-circuit, with initiation occurring in the hypothalamus leading to the secretion of gonadotropin releasing hormone (GnRH) in a pulsatile fashion. GnRH subsequently acts on the hypophyseal portal circulation influencing the anterior pituitary. GnRH-mediated pituitary activation results in secretion of luteinizing hormone (LH) and follicle-stimulating hormone (FSH). FSH acts on membrane receptors in the male Sertoli cells of the testes, whereas LH acts on membrane receptors in the Leydig cells in male testes, or the ovaries and adrenal cortex in females, to initiate the sequence of steps converting cholesterol to pregnenolone and finally to testosterone (Burger, 2002; Miller & Auchus, 2011; Nussey & Whitehead, 2001; Ramaswamy & Weinbauer, 2014; Stamatiades & Kaiser, 2018); (See figure 1).



**Figure 1.** Illustrating the hypothalamus-pituitary-gonadal axis. Green arrows indicate stimulating pathways, whereas red arrows indicate inhibition. Herein LH and FSH stimulate the synthesis of testosterone and spermatozoa, respectively, and moreover result in the downstream inhibition of the hypothalamus secretion of GnRH. Once testosterone levels fall adequately to no longer inhibit the hypothalamus, GnRH is released and the axis is re-enabled. This continues indefinitely in males to maintain testosterone and germ cell homeostasis. Figure is inspired by (Miller & Auchus, 2011; Nussey & Whitehead, 2001; Stamatiades & Kaiser, 2018).

### 2.0.1 Peripheral synthesis of androgens

Peripheral synthesis of androgens is also observed in bone and skeletal muscle, whereby local steroidogenic enzymes convert the steroid precursor dehydroepiandrosterone (DHEA) and DHEA-sulphate to active sex hormones (Aizawa et al., 2007; Vandenput & Ohlsson., 2010). In rats, a single bout of exercise is observed to increase both the metabolites and enzymes involved in this process (Aizawa et al., 2010). In bone tissue testosterone is mainly aromatized into estradiol, and acts as an important regulator of bone metabolism and remodeling (Vandenput & Ohlsson., 2010).

### 2.1 Testosterone in skeletal muscle

Notwithstanding mechanistic uncertainty, the literature propose that testosterone facilitate SkM hypertrophy and strength through augmentation of muscle protein synthesis (MPS); (Griggs et al., 1989), attenuation of muscle protein breakdown (MPB); (Braga et al., 2012; Ferrando et al., 2002),

improved amino acid reutilization (Ferrando et al., 1998), increased amino acid transporter mRNA-concentrations (Haren et al., 2011), increased satellite- and stem-cell commitment, proliferation and/or differentiation, all mediated through both AR-dependent and independent mechanisms (Bennet et al., 2009; Chen et al., 2005; Dubois et al., 2012; Herbst & Bhasin, 2004; Nelson et al., 2002). As previously mentioned, some mechanisms of testosterone action on SkM remain elusive, however, SkM, SCs, MSCs, and motor-neurons are all observed to have ARs which posit that the primary mechanisms likely are a result of cell-specific actions thereof (Chen et al., 2005; Dubois et al., 2012). Indeed, testosterone administration results in increased satellite cell number and myonuclei (Sinha-Hikim et al., 2002), a concomitant reduction in adiposity along with increased SkM mass (Corona et al., 2016; Wittert et al., 2003), and an increase in motor-neuron size and number (Dubois et al., 2012; Herbst & Bhasin., 2004). Moreover, testosterone is consistently shown to promote a dose-dependent increase in muscle size and strength in eugonadal men (Bhasin et al., 2001, 2005; Forbes, 1985; Sinha-Hikim et al., 2002), including significant improvements in hypogonadal males (Snyder et al., 2000; Wang et al., 2000). Collectively, testosterone have substantial effects on SkM mass and strength acting as a potent anabolic stimulant.

## 2.2 Testosterone pathways

Newly synthesised testosterone diffuses freely into the circulation where most (~40-60%) is bound tightly with sex hormone binding globulin (SHBG), the rest with albumin and a small amount remain in free-form. Free testosterone and testosterone loosely bound to albumin are deemed as bioavailable testosterone, the latter due to albumin readily dissociating during transit. The remaining (~40-60%) bound to SHGB is deemed non-biologically active (Nussey & Whitehead, 2001). Bio-active testosterone, a fat-soluble hormone, has five pathways: (i) The direct pathway (or traditional pathway), whereby testosterone diffuses across the cell membrane to bind with the androgen receptor (AR) in the cytoplasm (Bennet et al., 2009; Nussey & Whitehead., 2001), and (ii) the [direct-]amplification pathway, where the conversion of (~5-10%) testosterone to the more potent androgen dihydrotestosterone by 5-alpha-reductase occurs (Ishimaru et al., 1978; Nussey & Whitehead, 2001; Wilson, 2001). Both testosterone and DHT bind to ARs and shuttle into the nucleus where they stimulate transcription of various genes (Bennett et al., 2009; Prescott & Coetzee, 2006). (iii) The diversification pathway, a non-androgenic (i.e., estrogenic) pathway

which involves aromatization of testosterone into estradiol with mechanisms of action occurring in the bone and brain tissues (Cooke et al., 2017; Jones et al., 2006; Roselli, 2007; Russel & Grossmann, 2019; Simpson, 2004) acting in concurrence with the androgenic mechanisms of testosterone on these tissues (Venken et al., 2006; Zuloaga et al., 2008). (iv) The inactivation pathway, whereby the liver oxidises and conjugate testosterone to biologically inactive metabolites for renal excretion (Chouinard et al., 2008; Nussey & Whitehead, 2001; Zhou, 2008). Finally, (v) the indirect pathway [non-traditional], whereby testosterone stimulate signalling cascades independent of the traditional AR-complex, such as the Insulin-like-growth-factor I (IGF-I) pathway (Dubois et al., 2012; Hughes et al., 2016).

### 2.2.1 Traditional AR-genomic pathway (direct pathway)

The AR is a member of the steroid receptor superfamily of ligand-responsive transcription factors (Claessens et al., 2008; Evans, 1988). Inactive AR are associated with heat shock proteins (HSPs) and other chaperones along the cytoskeletal structures in the cytoplasm. HSPs complexed with cytoskeletal proteins (e.g., filamin-A) tether ARs to the cytoplasm. Once testosterone or DHT bind they induce conformational changes resulting in dissociation from HSPs, nuclear translocation, AR-dimerization with androgen response elements (AREs), and recruitment of various coactivators to facilitate gene-specific transcription (Bennett et al., 2009; Wyce et al., 2010). Within the nucleus, AR binds to tissue specific AREs facilitating recruitment of the general transcription machinery including histone acetyltransferases (HAT), enabling transcription of androgen-specific genes associated with the effects described previously (Bennet et al., 2009).

### 2.2.2 Indirect pathways

Hughes and colleagues (2016) investigated the direct and indirect pathway with inhibition models of AR and IGF-IR (insulin-like growth factor-1-receptor) respectively. Suggesting that the primary mechanism of action is mediated by the direct AR pathway rather than the indirect IGF-1R-PI3/Akt pathway for both young and aged/population expanded C2C12 cell lines on morphological measures of myoblast to myotube differentiation. Moreover, evidencing a heightened response to testosterone for the aged cell lines compared with the young. It also suggests that AR acts to maintain normal IGF-IR transcription, whereby inhibition of AR reduced IGF-IR transcription,

albeit testosterone-mediated increases provided no additional benefit, suggesting a ceiling. Thus, the direct AR-pathway seems to be the primary mechanism of action on skeletal muscle compared with the indirect IGF-IR pathway and its interactions (Dubois et al., 2012; Hughes et al., 2016). Importantly, the IGF-IR pathway is one of several indirect pathways' testosterone acts upon and, thus, these findings cannot account for all indirect, or non-traditional, effects.

### 2.2.2.1 “Non-traditional” actions of testosterone

Although the indirect pathways are likely not the primary mediator of testosterone's effects (Hughes et al., 2016), they still have a role to play. These pathways are characterized by (i) their speed of action, being mere seconds to minutes (e.g., intracellular  $[Ca^{2+}]$  upregulation), and (ii) being membrane mediated (e.g., membrane associated protein/receptor - signaling cascades), that are (iii) independent of the traditional AR-mediated transcriptional continuum (Bennett et al., 2009; Foradori et al., 2008). The latter notion is of importance, a caveat to the “non-genomic action” term often used, is how it negates the fact that many of these mechanisms do have downstream genomic effects (see below). A more appropriate term would be “non-traditional”, as this relates back to the direct AR pathway, and the fact that many of these “indirect” and “non-genomic” pathways are often both dependent on AR association with other complexes and offer genomic actions (see below).

### 2.2.2.2 Androgenic interaction with intracellular $[Ca^{2+}]$

The most consistent non-traditional mechanism of testosterone administration is the rapid and transient change in  $[Ca^{2+}]$  (Estrada et al., 2003; Foradori et al., 2008). Whether these changes in  $[Ca^{2+}]$  is due to ARs or with other membrane receptors is still uncertain, a phospholipase C and G-protein-coupled receptor mechanism has been suggested (Estrada et al., 2003). Regardless, alterations in  $[Ca^{2+}]$  can affect a myriad of pathways and mechanisms in SkM, of note is the calmodulin-dependent protein kinase (CaMK) pathway affecting the expression of several genes and signals involved in muscle regeneration, satellite cell recruitment, proliferation, and differentiation, and in promoting fiber type transitions through expression of nuclear factor of activated T cells (NFATc); (Tu et al., 2016). An additional pathway is through  $[Ca^{2+}]$ -induced

CaMK-Kinase-Alpha activation which is sufficient to activate mTORC1 and thus promote further SkM hypertrophy (Ferey et al., 2014).

### 2.2.3 Androgenic activation of secondary messenger pathways

In addition to  $Ca^{2+}$ -mediated secondary pathways, androgens are also shown to affect other secondary messenger pathways (SMPs) independent of the traditional genomic-pathway, albeit some remain dependent on other AR-complexes. A completely independent pathway is the previously mentioned IGF-I-PI3K-Akt-mTORC1 pathway (Hughes et al., 2014). Which result in increased protein synthesis and attenuated protein breakdown (Egan & Zierath, 2013; Hughes, 2014).

#### 2.2.3.1 Mitogen-activated protein kinase pathway (MAPK)

The AR-tyrosine kinase c-Src association also influence another SMP. C-Src is an upstream regulator of the MAPK (mitogen activated protein kinase) pathway, stimulating the ERK-2 (extracellular signal-reduced kinase-2) and Raf-1 components of the cascade (Foradori et al., 2008). Moreover, the previously mentioned IGF-1 pathway also activates MAPK-families which themselves are associated with a myriad of genomic actions affecting SM mass and strength (Egan & Zierath, 2013; Hughes, 2014). Testosterone administration in mice has shown activation of MAPK-p38 and inhibition of Jun HN2-terminal kinases (JNKs), the prior involved with differentiation of myogenic stem cells, and the latter a crucial regulator of apoptotic signaling (Brown et al., 2009). It is also postulated that there is a positive feedforward loop involving the steroid receptor coactivator (SRC) transcriptor family and MAPK-phosphorylation, whereby phosphorylation of SRC by MAPK increase their involvement and recruitment of coregulators for AR-mediated genomic effects. Thus, the AR-mediated SMPs stimulating MAPK act as an autocrine feed-forward to augment its genomic actions (Foradori et al., 2008). Brown (2009) also observed increased Notch-1 and 2 signaling with testosterone administration, which augments SC/MSK proliferation (Brown et al, 2009).

### 2.2.3.2 The myostatin pathway

The final relevant SMP involves crosstalk between the AR/ $\beta$ Catenin-complex and the Follistatin/Transforming Growth Factor- $\beta$  (TGF- $\beta$ ) signal pathways (Braga et al., 2012; Singh et al., 2009). Myostatin of the TGF- $\beta$  family is a familiar and potent negative regulator of SM growth and development (M. M. Chen et al., 2021), mediated through inhibition of SC/MSc proliferation (Taylor et al., 2001; Thomas et al., 2001), differentiation (Langley et al., 2002), and Akt/mTORC1 signaling (Rodriguez et al., 2011; Trendelenburg et al., 2009), whilst upregulating ubiquitin-proteasomal systems (Mcfarlane et al., 2006; Seiliez et al., 2013). Androgens thus, regulate myogenic differentiation through AR/ $\beta$ Catenin interaction, subsequent nuclear translocation to activate TCF-4 (T-cell factor-4) through the Wnt-cascade, and the resulting upregulation of follistatin (Fst); (Braga et al., 2012; Singh et al., 2009). Follistatin is shown to antagonize with several of the TGF- $\beta$  family, including myostatin and its inhibitory effects on SkM growth and development (Chen et al., 2021; Singh et al., 2009). Indeed, Mendler and colleagues (2007) demonstrated severe muscle atrophy and increased myostatin proteins in castrated rats, whereas testosterone administration reset myostatin levels equal to control. In total, the indirect/non-traditional effects of testosterone remain broad with substantial crosstalk, however, their respective magnitude of involvement in SkM adaptations remains to be determined.

### 2.3 Testosterone effects on satellite- and mesenchymal stem cells

Several of the traditional and non-traditional androgen pathways interact with SkM associated stem cells (Yue Chen et al., 2005; Dubois et al., 2012). Satellite cells are located between the basal lamina and plasma membrane of SkM fibers, typically in a quiescent state. During development and regeneration these cells become activated and enter the cell cycle where they proliferate before undergoing gradual differentiation to myoblast and finally, myotubes able to fuse with existing myofibers. Thereby providing both growth and novel myonuclei for the existing fibers, enabling homeostasis for the now larger 'myo-domain' (Almeida et al., 2016). Another population of AR-expressing quiescent stem cells are of mesenchymal origin, i.e., the MSCs, and serves as a reservoir for generating novel satellite cells able to enter both the myogenic and adipogenic lineages (Grounds et al., 2002). Both SC and MSCs are considered targets of testosterone due to their respective increase in both number (Sinha-hikim et al., 2003) and AR-concentrations with androgenic administration (Sinha-hikim et al., 2004). Thus, SC and MSC myogenesis, augmented

by testosterone, provide with novel myotubes and myonuclei for the growth and development of SkM whilst concomitantly increasing the AR-concentrations in a positive feed-forward for androgen sensitivity. Whether androgens act primarily on proliferation or differentiation is still a matter of debate (Dubois et al., 2012). Considering the intricate and broad involvement of androgens within the cellular machinery it is not unlikely that these mechanisms interact with cellular memory.

## 2.4 Overlapping signal transduction pathways between Testosterone and RT

Exercise is the most prescribed lifestyle intervention to promote health and longevity. Exercise facilitates a myriad of adaptations across all tissues of the body, enabling augmented strength, muscle mass, and cardiovascular fitness (Anderson & Durstine, 2019; Deschenes & Kraemer, 2002; Egan & Sharples, 2023). These adaptations are driven by exercise-induced signal transduction pathways that promote the tissues to adapt (Egan & Sharples, 2023). Of these signal cascades, several are shared with testosterone. As we have discussed earlier, beyond the traditional AR-genomic pathway, testosterone is also able to stimulate Ca<sup>2+</sup> related signalling pathways, MAPK, IGF-I, myostatin, and by stimulating SC and MSCs into increasing myonuclear abundance (Almeida et al., 2016; Braga et al., 2012; Dubois et al., 2012; Estrada et al., 2003; Foradori et al., 2008; Grounds et al., 2002; Hughes, 2014; Singh et al., 2009). Similarly, exercise alone also stimulate Ca<sup>2+</sup> signalling, MAPK, IGF-1, and myostatin (Egan & Sharples., 2023). RT and testosterone likely offer activation of these pathways at differing magnitudes. Nevertheless, they are shared. Thus, considering the intricate involvement of testosterone and its metabolites within the cellular machinery, it is not unlikely that these mechanisms interact with SkM memory akin to that observed by RT alone (as described below).

## 2.2 Skeletal muscle memory

Several resistance- training, detraining, and retraining models (TDR-model) in humans consistently shown SkM to have memory mechanisms maintaining both mass and strength (fitness) despite extensive detraining (12-32 weeks) when compared with baseline (Bickel et al., 2011; Blocquiaux et al., 2020; Henwood & Taaffe, 2008; Psilander et al., 2019; Seaborne et al., 2018; Staron et al., 1991). Moreover, these mechanisms facilitate a faster return to, and exceeding



of, fitness levels observed after the initial training phase. Most returning to previous fitness levels within half the time of the initial training (Blocquiac et al., 2020; Henwood & Taafee., 2008; Psilander et al., 2019; Seaborne et al., 2018; Staron et al., 1991). Indeed, suggesting a return to fitness within 2-5 weeks (Blocquiac et al., 2020; Psilander et al., 2019; Seaborne et al., 2018). Between 32 weeks to a full year is necessary to completely ablate this memory mechanism and its effect on retraining (Bickel et al., 2011; Correa et al., 2016; Ivey et al., 2000). However, Snijders and colleagues (2019) observed that despite 52 weeks of detraining (i.e., returning to autonomous movement) in older adults, strength was partially preserved. Albeit any gained SkM mass was completely abolished. Furthermore, only a fraction of the training condition volume is necessary to either attenuate any decline ( $1/9^{\text{th}}$  of volume) or possibly continue adaptation ( $1/3^{\text{rd}}$  of TC-volume). However, the participants in this study were untrained, which likely lowers the training volume needed to maintain fitness (Bickel et al., 2011). Collectively, the literature consistently shows a strong memory mechanism of fitness and trainability because of RT.

Discussed herein are the two primary theories of such a SkM memory mechanism; myonucleic permanence and epigenetic memory (Seaborne et al., 2018; Sharples, Stewart, et al., 2016; Tim Snijders et al., 2020). The myonuclear permanence theory is largely built by animal models in rodents, with some contradictory results and uncertainty in human models, mainly due to poor methods and measurements (Snijders et al., 2020). Nevertheless, studies from Bruusgaard (2010) and Egner (2013) both provide with strong evidence supporting myonuclear permanence in rodents. Evidence in humans suggests that myonuclei are not retained throughout the lifespan, although the literature is conflicting (Snijders et al., 2020). Currently, Psilander (2019) and Blocquiac (2020) are the only two studies directly investigating the myonuclear permanence hypothesis in a TDR-model. Neither corroborate the hypothesis in humans, as myonuclei remained unchanged when standardized with fiber type cross-sectional area (CSA) during the training conditions. Nor did they observe any change in myonuclear domain size (I.E., myofiber area per myonuclei remained constant). Blocquiac (2020) observed a significant decrease in myonuclei during detraining, which Psilander (2019) only saw a tendency for. However, limitations in these studies pose a challenge to their validity. Both Psilander (2019) and Blocquiac (2020) failed to achieve any increase in myonuclei at any point during the training intervention, limiting the findings severely. Furthermore, both are limited by untrained participants, whereby Blocquiac (2020) recruited older individuals in their study, a population known to have decreases in anabolic

adaptability with concomitant reductions in satellite cell and myonuclear abundance (Burd et al., 2013; W. Chen et al., 2020). A recent observational study investigating myonuclear permanence in previous and current anabolic users, compared with non-users, found no significant difference in myonuclear number per area muscle fiber. Once again limited, with a poor sample size in the steroid groups (Lima et al., 2022). However, a similar observational study in elite powerlifters showed that previous anabolic steroid users had significantly more myonuclei per fiber in certain fibers of the trapezius muscle (Eriksson, 2006).

Thus, based on contemporary literature there seems to be a lack of consensus on the existence of myonuclear permanence in human SkM, with a call for novel experiments to elucidate further. Contrarily, investigations into epigenetic muscle memory have provided clearer insights (Seaborne et al., 2018).

## 2.3 Epigenetics

From botanical breeding of plants in the late 1800s to chromosomes, the discovery of DNA, and non-coding RNA, to nucleosomes and chromatin in the 1900s. Genetics have taken far leaps the past two centuries. It is not until the beginning of the new millennium that the modern notion of *Epigenetics* would have its turn in the spotlight (Deichmann, 2016; Gayon, 2016). The contemporary term epigenetics relates to chemical modifications to DNA that alter the expression of its genes without altering the base-structure of the DNA-strand itself (Deichmann, 2016). The primary mechanisms of epigenetic modifications to DNA that alter gene-expression are: (i) Histone modifications (i.e., chromatin remodeling), (ii) non-coding RNA-based mechanisms, and (iii) DNA methylation (Egan & Sharples., 2023).

### 2.3.1 Histone Modifications

The base units of the Chromatin, nucleosomes, are composed of a histone octamer protein with an associated DNA-strand coiled around by virtue of hydrogen-bonds to each of its protein subunits (H2A, H2B, H3, and H4). The histone subunits have N-terminal tails protruding outward which are susceptible to chemical modifications that alter their affinity for the DNA-strand. Covalent modifications such as methylation, acetylation, and phosphorylation make up the most characterized chemical modifications. Along with other ATPase-enzymes, known as chromatin

remodeling complexes, the chromatin may be either condensed (i.e., repressing genes) or decondensed (i.e., expressive); (Alberts et al., 2015; Gibney & Nolan, 2010).

### 2.3.2 Non-coding RNA

RNA-based epigenetic mechanisms (i.e., non-coding RNA such as microRNAs) are less understood, albeit likely involved in transcription and translation, with some crosstalk between non-coding RNA and DNA methylation (Gibney & Nolan, 2010). They are most understood as post-transcriptional controls, acting as riboswitches, mRNA-inhibitors, immune-response elements, and as protein-like catalyst or scaffolds (Alberts et al., 2015). microRNAs have recently been implicated in the regulation of myoblast proliferation, differentiation, and cell fate determination, and is shown to be a component of AR-induced gene expression (Wyce et al., 2010).

### 2.3.3 DNA Methylation

The reversible covalent modification of the 5'-position cytosine-phosphate-guanine dinucleotide (CpGs) of the DNA strand, mediated by DNA methyltransferases (DNMTs). Once the CpGs are methylated, the chemical characteristics of the DNA-strand near the site is altered. Generally, the acquisition of methyl-groups on CpG-sites (hypermethylation) near gene-promoters result in gene repression, by either inhibiting proteins in recognizing the DNA or the attraction of other repressive proteins (Gibney & Nolan, 2010). Interestingly, CpG base-pairing occurs at a statistically lower frequency than expected throughout the genome, occurring more frequently in clusters termed CpG-islands (Gardiner-Garden & Frommer, 1987). These CpG-islands are distributed somewhat unevenly throughout the genome, with about half located near promoter-regions and the remainder intragenically (Illingworth et al., 2008). Furthermore, about 80% of CpGs outside island clusters are methylated, whereas the CpG-islands typically have lower levels of methylation (Shen et al., 2007). All forms of epigenetic modifications can be either highly transient or heritably fixed, with some lasting mere hours to weeks, whereas others are retained into the next line of daughter cells, possibly lasting throughout the lifespan, and passed along to the next generation (i.e., transgenerational epigenetics); (Barrés et al., 2012; Gibney & Nolan, 2010; Kangaspeska et al., 2008; Ng & Gurdon, 2008; Sharples, Stewart, et al., 2016; Verhoeven et al., 2016; Yuta et al., 2023).

### 2.3.4 Epigenetic skeletal muscle memory

Sharples and colleagues (2016) discovered that C2C12 SkM cells have an epigenetic memory of previous exposure to TNF- $\alpha$  (Tumor necrosis factor - alpha), whereby the early-life exposure increased their susceptibility to impaired differentiation in later proliferative stages. Evidencing retained myoD methylation after 30 population doublings. Thus, suggesting DNA-methylation as an important regulator of myogenic genes throughout the SM cell proliferative stages. Another study investigating aged human SkM cells and their ability to self-renew, showed impairment in this ability along with higher overall DNA-methylation. Interestingly, demethylation treatments in cultured cells facilitated improvement in this regenerative ability. Particularly, showing demethylation of a specific gene associated with self-renewal and quiescence (SPYR1), which when knocked out abolished any effect of the demethylation treatment on self-renewal (Bigot et al., 2015). Within the exercise continuum, endurance type exercise has consistently shown alterations in the mitochondrial biogenesis epigenome, once sufficient volume or intensities are reached, affecting histone modifications and DNA methylation both acutely and chronically (Ntanasis-Stathopoulos et al., 2013). Following this, Seaborne and colleagues (2018) first reported an epigenetic SkM memory mechanism in a human TDR-model. Identifying several genes displaying retention of DNA methylation even into detraining following a period of training. Furthermore, some genes demonstrating hypomethylation in response to earlier training demonstrated even greater hypomethylation upon later retraining and was associated with the largest increase in gene expression. The genes identified by Seaborne (2018), were integrated with hundreds of transcriptomic profiles in SkM in response to acute and chronic RT. Here they identified five genes with concomitant epigenetic and transcriptomic retention due to both acute and chronic RT. All of which were associated with extra cellular matrix and actin remodeling, mechano-transduction and TGF- $\beta$  signaling (Turner et al., 2019). This epigenetic memory mechanism was further corroborated in a mouse TDR-model, which also discovered a nucleus-specific memory mechanism. Comparing interstitial nuclei with myonuclei, they discovered that these nuclei were reciprocally regulated, and furthermore, corroborated the findings of Seaborne (2018), evidencing a global hypomethylation pattern due to exercise, in both nucleus-types. Furthermore, confirming several genes to have retentive methylation across the detraining condition. Interestingly, with respect to the Wnt signaling pathway they discovered differential

methylation, with myonucleic hypomethylation and interstitial hypermethylation (Wen et al., 2021). Indeed, the epigenome trends toward promoter hypomethylation in genes associated with metabolism, myogenesis, contractile activity and oxidative stress resistance, when comparing healthy adult men with lifelong elevated physical activity and sedentary individuals of the same age (Sailani et al., 2019). Accordingly, prenatal stressors, physical inactivity, and unhealthy diets, are all associated with specific detrimental epigenetic modifications (Beiter et al., 2020). Collectively, SM consistently show to possess a memory mechanism in both the macro and micro scale. With new evidence pointing out epigenetic modifications having such retentive abilities. The genes involved should therefore be explored in depth to elucidate their mechanisms of action in SkM.

#### 2.4 Evidence for SkM memory of previous testosterone use

To the authors knowledge, only one study has investigated the potential memory mechanisms of testosterone (Egner et al., 2013). Egner and colleagues (2013) demonstrated that 2 weeks of testosterone administration in female mice resulted in an acute CSA increase and a chronic increase in myonuclei far surpassing sham. Moreover, this increase in myonuclei was retained for the following 15 weeks, whereas the initial increase in CSA returned to baseline within 3 weeks. After this period, the mice were exposed to overload, whereby the steroid group had significantly more hypertrophy compared with sham. This gap between initial administration and overload accounted for about 12% of mouse lifespan, which would translate to a decade in a human equivalent.

Considering that humans and mice display differing adaptations in myonucleic retention due to RT (Blocquiaux et al., 2020; Bruusgaard et al., 2010; Egner et al., 2013; Gundersen, 2016; Psilander et al., 2019), and as previously discussed, observational studies investigating previous anabolic steroid users found differing results in myonucleic abundance (Eriksson, 2006; Lima et al., 2022). It becomes increasingly important to discern whether the mechanisms observed in rodents also hold true when humans are exposed to exogenous testosterone. Furthermore, no studies have investigated whether testosterone facilitates epigenetic memory mechanisms recapitulating those observed by RT (Seaborne et al., 2018).

## 2.5 Implications for sports, doping, transgender athletes, and the ageing population

The isolation of testosterone in 1935 led to the initial rise in the use of anabolic androgenic steroids (AAS) for performance enhancement and muscular growth among athletes and bodybuilders (Hoberman & Yesalis, 1995; Kanayama et al., 2018). This resulted in nations utilizing testosterone and other AAS to propagate representative athletes in international sports, with the USSR initiating the trend and the USA reciprocally doping their athletes in systematic fashion. Which, eventually, from the 1980s and onward resulted in the general public gaining “underground” access (Kanayama et al., 2018). Despite the International Olympics Committee (IOC) banning stimulants as early as 1967 and AAS in 1976, nations and athletes continued use of both and avoided detection by strategically dosing far in advance of any tests (Kanayama et al., 2018; Ljungqvist, 2012). However, the IOC could only regulate for Olympic events, which left most sporting events in the hands of international federations and national association, which remained surprisingly idle until the International Association of Athletics Federations (IAAF) developed an immunological method of detecting AAS, which was employed in 1974 for the first time. Although, the methods improved, testing at competition only was a major limitation. Thus, employing controls during training seasons was implemented in 1980-1990. Shortly after, the World Anti-Doping Agency (WADA) was created in 1999 (Ljungqvist, 2012). In present times, there is a growing and widespread use and abuse among athletes and non-athletes alike, despite controls, with the emergence of new drugs and methods of concealment which the WADA consistently must develop methods to test (Kanayama et al., 2018; Ljungqvist, 2012). The prevalence of AAS use among athletes, despite years of battle and education is still estimated to be around 14-39%, which is far above the estimates derived from doping controls (1-2%); (Hon & Kuipers, 2015). Thus, it seems that doping controls are severely inefficient in detecting current or previous AAS use. Moreover, athletes caught with any of the prohibited substances in their system may be sentenced ineligible to compete from 1 month up to 4 years, depending on the severity of violation. Recurring violations may result in a lifetime ban (WADA, 2021). The implications of a memory mechanism of previous testosterone, and likely other androgens, is multi-faceted. Firstly, the ineligibility sentences could be dramatically increased, and second, novel detection tests may be created to discover whether athletes currently or previously used AAS. Which could result in the dramatic uncovering of the remaining 13-38% of potential users estimated by de Hon (2015), and of the likely large number of people that have ever used AAS.

Furthermore, in recent years the traditional binary categorization of male and females are challenged, with an increasing proportion of trans-gender athletes. Determining the eligibility of trans-athletes, particularly trans-females (previously male females), has gained controversy (Hamilton et al., 2021). The implications of a testosterone memory mechanism would indeed pose a major challenge to the inclusion of trans-females into traditionally cis-female sporting events, as the years of previous exposure could result in a lifetime benefit to these athletes.

With age there is an observed decrease in testosterone, concomitantly followed with age-related declines in physical health (Barone et al., 2022; Basaria, 2013). Episodic treatment with testosterone in mid- to late life, given a memory mechanism, could thus, provide with a novel strategy to attenuate this decline in physical prowess with age. Especially considering episodic treatment have potentially less adverse effects (Barone et al., 2022). Finally, understanding the mechanistic underpinning of testosterone's actions would illuminate our understanding of this hormone and provide with insights into ways to optimize its homeostasis for health and longevity.

## Part III - Methodology

### 3.0 Cell culture as an in vitro model of skeletal muscle

The current ethical position on the use and risks associated with testosterone administration in humans (Bassil et al., 2009; Grech et al., 2014) limits the design and support for human studies investigating the potential memory mechanisms of this hormone. Cell culture models are often used as an alternative to human or animal studies for this reason. These models allow researchers to control experimental conditions, manipulate variables, and isolate factors or pathways with precision and accuracy. Moreover, cell culture models reduce ethical concerns associated with animal and human studies, as well as substantially lowering the costs associated with such research. Another advantage is the reproducibility of results, whereby experiments are easily replicated, standardized, and scalable. Additionally, cell culture offers convenience and flexibility for the researchers by being more easily maintained and manipulated than living organisms, enabling experiments to be performed at any time and for longer periods. However, limitations are present in these models as well. Keeping high quality standards and protocols to maximize

reproducibility is essential for the success of this model and is often a challenging task. Finally, no cell culture model can accurately represent the complexity of living organisms and should therefore be interpreted with this caveat in mind (Allen et al., 2005; Hirsch & Schildknecht, 2019; Juan-Manuel et al., 2013; Langhans, 2018).

### 3.0.1 C2C12 Skeletal muscle myoblasts

The C2 cell line was initially developed by Yaffe and Saxel (1977) using crushed adult C3H mouse leg muscles to promote the proliferation of satellite cells. These cells were later found to undergo spontaneous differentiation into myotubes with serum withdrawal and do not require additional growth factors to facilitate this process. This process recapitulates the differentiation observed in human SkM cells. Thus, making C2 cell lines a valuable tool for studying skeletal muscle development and regeneration in both animals and humans (Blau et al., 1985). Moreover, C2C12 cells, a subclone of the C2-line, share and express many of the genes and proteins found in human SkM cells, including key transcription factors and myosin heavy chains. This shared gene expression profile between humans and C2C12 therefore enables meaningful comparisons between the two systems, and allow translation of findings derived from basic research to clinical applications (Allen et al., 2005). Additionally, C2C12 cells are all clones (i.e., derived from the same parent cell), sharing an identical genome, and therefore, removes genetic variability (Yaffe & Saxel, 1977). This allows researchers to reduce the n-number substantially whilst maintaining appropriate power (Serdar et al., 2021). Finally, C2C12 cells have the primary characteristics of cell culture models as described above (6.0) and are therefore a highly valuable model system for studying human SkM.

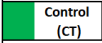

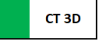


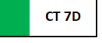


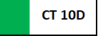

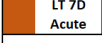

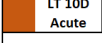



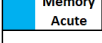



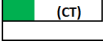

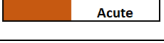


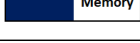
## 3.1 Methods

### 3.1.1 Study design

The design includes a total of twelve individual 6-well plates to satisfy condition time-points and isolations. These were assigned into six conditions as seen in figure 2. These are: Control (CT), Early acute testosterone (ET), Late testosterone (LT), LT acute testosterone (LT Acute/LTA), Early + Late testosterone (Memory/ME), and Early + Late acute testosterone (Memory Acute/MA). Each 6-well provided 2-wells for DNA, RNA, and microscopy, each. This experiment was ultimately completed N=2 in triplicate for morphology (three images per plate) and in



duplicate for RT-PCR (2-wells per plate). Ideally, striving for N=3, however limitations in time and laboratory issues led to N=2 only being possible (see 10. limitations).

CONDITIONS		Protocol			
		Day 0	Day 3	Day 7	Day 10
		ISOLATE			
 		DM only	4H DM => Isolate 4H Testo => Isolate		
 		DM only	DM 4H Testo => DM to 7D	4H fresh DM => Isolate	
 		DM only	DM 4H Testo => DM to 7D	DM only	Isolate
		DM only	DM only	4H Testo => Isolate	
		DM only	DM only	4H Testo => DM to 10D	Isolate
		DM only	DM only	Testo => leave to 10D *	Isolate
		DM only	4H Testo => DM to 7D	4H Testo => DM to 10D	Isolate
		DM only	4H Testo => DM to 7D	Testo => leave to 10D *	Isolate
					

**Figure 2:** Study design schematic indicating all time-points, isolations, treatments, and conditions. A total of 12 individual 6-well plates are employed to satisfy the design parameters. \* Indicates testosterone treatment being left on until next timepoint, all other testosterone treatments are left for 4 hours (H), washed, and resuspended in fresh DM required for the following time point. At day 0, all conditions are treated with DM to initiate differentiation from proliferating myoblasts into myotubes and marks the beginning of the experiment. The bottom row illustrate each individual condition assigned from the 12-plates.

### 3.1.2 General Cell Culture

#### 3.1.2.1 C2C12 Skeletal Muscle Myoblasts

Our laboratory obtained commercially available C2C12 cell lines (Sigma-Aldrich, ECACC, UK), a subclone of the C2 line (Blau et al., 1985; Yaffe & Saxel, 1977), and stored them in liquid nitrogen (LN2). Population doublings from obtained C2C12 lines before inclusion to the experiment ranged from P5 to P7, and was dependent on number of cells needed, their confluency, and current number of cells in culture.

### 3.1.2.2 Tissue Culture Reagents

Sterile cell grade culture medias and supplements were acquired as follows: Growth media (GM), composed of Dulbecco's modified Eagle's medium (DMEM); (Gibco, USA), 10% heat-inactivated fetal bovine serum (HI-FBS; Gibco, USA), 10% heat-inactivated Newborn Calf Serum (HI-NBCS; Gibco, USA), 1% Penicillin-Streptomycin (PenStep; Gibco, USA) and 1% L-glutamine (Gibco, USA). Two Differentiation medias (DM) were made, (i) DM-T: composed of DMEM, 2% horse serum (Gibco, Waltham, MA, USA), 1% Penicillin-Streptomycin, and 1% L-Glutamine, made to later be aliquoted testosterone to a concentration of 100 nM (see 8.3.1). (ii) DM-DMSO: aliquoted 0.002% dimethyl sulfoxide (DMSO; Fischer BioReagents, USA) as a vehicle control for testosterone (see 8.3.0). Phosphate buffered saline (PBS; HyClone, USA). Gelatin solution, composed of 0.2% of Porcine Gelatin type A (Sigma-Aldrich, USA) mixed with HyPure Cell culture grade water (HyClone, USA). 4% Paraformaldehyde solution for cell fixation, was composed of 4 grams of paraformaldehyde powder (Sigma-Aldrich, USA) in 100 ml PBS and pH adjusted using HCL, NAACL, and a pre-calibrated benchtop pH-meter ( ) to a pH of 7.4.

### 3.1.2.3 Cell counting by Trypan Blue Exclusion

Cell counting was performed using a hemocytometer, made of a glass cover slip resting on a counting chamber. Cell suspension was homogenized and prepared by diluting a 1:1 suspension to 0.4% trypan solution (Gibco, USA). This solution was dispensed into the counting chamber and each cell contained within the appropriate grids was counted. Viable cells were discerned by their size, shape, and visibility, whereby misshapen, overly large, or trypan blue positive cells were excluded. The hemocytometer contains four grids to count, if the standard deviation between either of the 4 grids was high a recount was performed. The average of the four grids, representing the mean number of cells present in  $0.1\text{mm}^3$  served as the basis for calculating the mean number of cells pr ml of suspension. This counted value multiplied by 2, accounting for the trypan dilution, and further multiplied by  $10^4$  to account for the dispersion within the grid volume, results in the total number of cells contained per ml. Multiplying this with the suspension total volume and the total cell count is presented. This count is then used to calculate the dilution needed to reach 80 000 cells per ml.

#### 3.1.2.4 Cell culture

A microbiological safety cabinet (Thermo Scientific, USA) was used for all cell culture work. C2C12 (Sigma-Aldrich, ECACC, UK) were brought up from LN<sup>2</sup> storage in 2.0 ml cryovials at  $1 \times 10^6$  cells.ml(-1), and left to thaw at room temperature. Once thawed, cells were seeded at  $1$  to  $2 \times 10^5$  cells (0.5-1.0 million cells) per T75 flask. T75s were pre-gelatinised with 6 ml of 0.2% gelatin, which was left at room temperature for 10 min and another 10 min in the incubator at 37°C, before aspirating off excess gelatin. 14 ml Growth Media (GM) was added to the T75 prior to aliquoting the cell suspension (totalling 15 ml) to ensure even distribution across the flask. Incubation of all cells occurred in a 37°C humidified 5% CO<sub>2</sub> atmosphere incubator (Fisherbrand, Isotemp, UK).

Once cells reached 80% confluency after about 48-72 hours, they were washed 2X with PBS to remove serum (serum inhibits trypsin) and trypsinised using 1 ml 0.05% trypsin-EDTA (Gibco, USA). Trypsin was left on for 5 min in the incubator. Disassociation of cells from gelatin was observed under the microscope (Motic AE2000, MoticEurope, Spain). 4 ml of GM was added to neutralize trypsin. The now 5 ml solution in the flasks were used to rinse off cells by pipetting up and ejecting the solution whilst inclining the flask to ensure all cells were collected. Once collected the cells were homogenized using an 18-gauge needle and syringe to prevent clustering. 15  $\mu$ l cell suspension was aliquoted 1:1 with trypan blue stain and dispensed into a haemocytometer for cell counting (see 8.2.4). Cells were then seeded at 2 ml of 80 000 cell/ml suspended in GM (totaling 160 000 cell/well) in individual pre-gelatinised 6-well plates and cultured until reaching a confluency of 70% (figure 3.). Any remaining cells from the suspension was cryopreserved.

C2C12 cells ready for differentiation (70% confluent) had their GM aspirated, washed twice by 1 ml PBS and aliquoted 2 ml of DM to initiate differentiation. This point denotes the 0-hour time point and serves as the start of the experiment.

#### 3.1.3 Cell Treatment

At the 0H time point the first control condition (CT) was isolated as described below. All other conditions were left to incubate in DM for the following 72 hours (see figure 2).

Each time point has one to three conditions to treat; (i) media change, (ii) testosterone exposure, and (iii) isolation, performed in this respective order. (i) media change is performed by aspirating DM, performing a 2x PBS wash, and re-aliquoting 2 ml fresh DM. (ii) Testosterone was reconstituted prior to experiments (see 8.3.1) and relevant conditions were washed 2x PBS before aliquoted 2 ml of 100nM Testosterone in DM and left on for 4 hours or until next time point depending on condition. After 4 hours, media was aspirated, and cells were washed 2x PBS. Then the cells were aliquoted 2 ml DM until next time point or prepared for isolation (see figure 2).

(iii) The Isolation procedure starts by taking 3x images at 4X and 10X, respectively, using a camera attachment (Moticam x3, Motic Europe, Spain) to an inverted microscope (Motic AE2000, MoticEurope, Spain). Relevant wells for IHC and imaging are aliquoted 750  $\mu$ l of 4% PFA solution (see 8.2.3) and left in room temperature for 10 minutes. After which PFA was aspirated off and 2 ml PBS was added to prevent dehydration of the cells whilst storing for later processing (see 8.4.2). Following this, cell extraction for DNA isolation were suspended in 230  $\mu$ l PBS and 20  $\mu$ l protein kinase A (PKA); (250  $\mu$ l total for all wells), and mechanically assisted by using a cell scraper to collect and transfer all cells across all wells into a 2 ml eppendorf for later processing (see 8.5.2 and 8.5.3). Cells for RNA isolation were suspended in 300  $\mu$ l in each well (600  $\mu$ l total), mechanically collected and stored in the same fashion as DNA for later processing (see 8.5.1) for RNA isolation. Finally, the plates containing the fixed cells were covered in parafilm and stored in fridge until later processing (see 8.4.1).

### 3.1.3.1 Testosterone reconstitution

The rationale behind 100nM testosterone concentration is derived from Hughes (2016), where 500nM testosterone is shown to have the same effects as 100nM, indicating saturation of C2C12 AR-receptors at this concentration. Furthermore, 4 hours is in theory sufficient for AR-translocation and subsequent gene expression to occur. The AR already bound by testosterone will nevertheless perform their duty despite washing as these are already taken up within the cell membranes. Most changes in methylation post exercise are also observed to occur between 30 min to 3 hours after a 45 min bout of RT (Gorski et al., 2023; Maasar et al., 2021; Seaborne et al., 2018; Sexton et al., 2023). Thus, 7.2 mg of Testosterone (T0027; TCI Europe, Belgium) was dissolved in 5 ml DMSO at a concentration of 5mM Testosterone. This was further aliquoted into 50  $\mu$ l working stock tubes and frozen down to ensure minimal degrading over time. For each time point,

the exact amount of Testosterone was calculated and made up from the working stock. E.g., for the 3 Day time point 70 ml of 100nM testosterone diluted in DM was required. From the working stock 1.4  $\mu$ l was extracted and diluted in 14 ml of DM, making a concentration of 500 nM. This was then diluted in a 1:5 ratio, with 56 ml DM, making up 70 ml total of 100nM testosterone in DM. This testosterone solution also contains about 0.002% DMSO. Which is the basis of the rationale for dosing all other conditions with a 0.002% DMSO vehicle in their respective DM.

### 3.1.4 Morphological Analysis

Images collected as described above (8.3.0) were used for morphological analysis. Whereby the 3 images at 10X magnification (totaling 6 images per condition) were pooled into a mean  $\pm$  SD of myotube numbers, diameter, and area, respectively. Analysis was performed by ImageJ software (Java software, National Institutes of Health, USA). Myotube number was assessed by counting the total myotubes observed within each image, with the inclusion criteria for a count being a myotube containing at least 3+ nuclei within the cell membrane. This avoids miscounting cells undergoing mitosis. Myotube diameter was calculated by measuring 3 equidistant points along the length and across the width of a myotube. Myotube area ( $\mu$ m<sup>2</sup>) was measured by manually outlining myotube membranes using the “freehand selection” tool. During imaging, the Motic software (Motic Images Plus 2.0, MoticEurope, Spain) attach a scalebar which is used as reference to convert pixels to  $\mu$ m using ImageJ.

#### 3.1.4.1 Fused and branching myotubes, “myobranches”

The cells in this experiment were strong differentiators compared with other batches in our laboratory. This resulted in the occurrence of myotube branching (see figure 6B), whereby myotubes fuse together to form large branching complexes. These “myobranches” are magnitudes larger than the average “normal” myotubes and increase the spread in the data as observed by the large SDs. They also posed a difficulty in the diameter measurements as their variability in shape made them ineligible for accurate diameter measurements. Thus, they were excluded from all diameter data. However, for area analysis these are presented in an individual myobranche analysis.

### 3.1.5 RNA isolation and RT-QRT-PCR

#### 3.1.5.1 RNA isolation

Samples collected during isolation (8.3.0) were removed from the freezer, vortexed, and left to thaw at room temperature for 10 min. Following this, all samples were placed on ice to preserve RNA integrity. 200ml chloroform per 1 ml of Trizol was aliquoted to the samples (120  $\mu$ l chloroform for 600  $\mu$ l Trizol) and left in room temperature to incubate for 2-3 minutes. Samples were then centrifuged (Heraeus Fresco 17, Thermo Fisher, USA) at 12 000G for 15 min at 4C. This result in phase separation of the RNA and Trizol/protein contents, whereby the transparent RNA-phase was carefully collected and aliquoted to an RNase-free eppendorf. The remaining phases were discarded. The RNA was aliquoted 300  $\mu$ l isopropanol, vortexed, and left to incubate in room temperature for 10 minutes before centrifugation; at 12 000g, 4C for 10 minutes. After which the sample contains an RNA-pellet and a clear supernatant, the latter being removed without disturbing the former. The RNA-pellet was then washed with 600  $\mu$ l 75% Ethanol (VWR Chemicals, USA) and centrifuged at 7500g for 8 min at 4C. The remaining ethanol was aspirated out and the RNA-pellet was air dried to ensure no remaining ethanol. Finally, the pellet was re-suspended in 32  $\mu$ l RNAase free TE buffer (Invitrogen, Thermo Scientific, USA).

#### 3.1.5.2 RNA quantity and purity

The quantity and purity of RNA was determined using spectrophotometry (QIAxpert, Qiagen, Germany). Whereby each sample was vortexed to homogenize, then 2  $\mu$ l of sample was aliquoted to a loading slide. The loading slide was inserted into the machine whereby the QIAxpert software enables allocation of sample names and blanks. The concentration of RNA given in ng/ $\mu$ l was recorded and used to calculate appropriate master mix for rt-qrt-PCR.

#### 3.1.5.3 Reverse transcription quantitative real time polymerase chain reaction (RT-qRT-PCR)

The reverse transcription of isolated RNA was performed using a Rotorgene 3000Q (Qiagen, UK) and Rotorgene software (Hercules, USA). The master mix solution was prepared using 5ul Quantifast<sup>TM</sup> SYBR Green, 0.075  $\mu$ l Forward Primer, 0.075  $\mu$ l Reverse Primer, and 0.1  $\mu$ l Quantifast Reverse Transcriptase mix, totaling 5.25  $\mu$ l master mix per sample. The RNA sample was diluted to 7.37 ng/ $\mu$ l. Both the master mix and RNA samples were then aliquoted as 5,25  $\mu$ l and 4,75  $\mu$ l, respectively, to individual Strip Tubes (Qiagen, Hilden, Germany) totaling 10  $\mu$ l per sample. All samples were run in duplicates. Rt-qPCR was run with the following settings: Initiated

by (i) 10 minutes at 50C for reverse transcription and synthesis of cDNA, (ii) 5 minutes at 95C for transcriptase inhibition and initial denaturation, (iii) 45 cycles of 10 seconds at 95C for annealing, and 30 seconds at 60C for extension.

Once completed a melt curve analysis, amplification efficiency, and Ct-value consistency (SD  $\pm$  0.25) across duplicates, determined which samples were eligible for exclusion and re-run. Mean amplification efficiency for the housekeeping gene RP-IIb was  $94 \pm 3.7\%$ . mRNA expression was quantified for the myosin heavy chains (MHCI, MHC2, MHC4, and MHC7), and the Androgen Receptor (AR), to support the changes observed in myotube morphology at the molecular level. Exclusion criteria for target genes mean amplification efficiency was set to be  $>10\%$  to that of RP-IIb, and an average efficiency across duplicates  $\geq 90\%$  with a SD  $\geq 0.15$ . Target genes mean efficiencies were for the AR  $92 \pm 2.6\%$ , MHCI  $95 \pm 3.9\%$ , MHC2  $94 \pm 3.7\%$ , MHC4  $97 \pm 7.3\%$ , and MHC7  $95 \pm 4.2\%$ . mRNA expression was quantified using the ( $2^{-\Delta\Delta Ct}$ ) method (equation 1), using RP-IIb as reference gene and calibrator for the control treatment (CT) at 0H (equation 1B); (Livak & Schmittgen, 2001). Mean Ct-value of RP-IIb was  $18.84 \pm 0.46$ , variation = 2.42%. For target gene  $\Delta\Delta Ct$  calculation, the mean  $\Delta Ct$  for CT at the 0-hour time-point was initially set as calibrator. However, because the cells at 0-hours were still proliferative and not yet terminally differentiated (G0), there is a possible confound in using a cell population mostly within the cell cycle as baseline for cells mostly in G0. Moreover, the purpose of the experiment is to model adult organisms, therefore, the calibrator was also set as CT at the 3-day time-point within the target gene (equation 1B). Whereby both calibrations are presented where relevant within the analysis.

$$A: \Delta Ct_{Target Sample} = (\bar{x}Ct_{Target Sample} - \bar{x}Ct_{Housekeeping Gene})$$

$$B: \Delta\Delta Ct_{Target Sample} = (\Delta Ct_{Target Sample} - \bar{x}\Delta Ct_{Calibrator})$$

$$C: Fold change = (2^{-\Delta\Delta Ct_{Target Sample}})$$

**Equation 1:** The ( $2^{-\Delta\Delta Ct}$ ) method showing the sequential order to quantify mRNA expression of target genes from raw Ct-values. **A:** Depicts how the  $\Delta Ct$  of individual samples is calculated using the mean of the housekeeping reference gene RP-IIb. **B:** Follows with the next step by calculating the  $\Delta\Delta Ct$  of a target sample using the mean of the Calibrator (control condition at baseline/0-hour). **C:** Shows the final step in deriving the fold change of mRNA expression of target genes by raising 2 to the negative power of the  $\Delta\Delta Ct$  of a target sample (Livak & Schmittgen, 2001).

### 3.2.0 Statistical analysis

All processing and statistical analyses are completed with R 4.2.2 and R Studio (RStudio 2022.07.02 build 576). Values presented are mean and standard deviation, unless otherwise specified. Morphological data processing and analysis indicated non-normal distribution of several combinations of data. Histogram, QQ-plot, residual plot, kurtosis, skew, and a Shapiro-wilks normality test confirmed this. Due to these appearing mostly as deviating normality by skew, a positive kurtosis, heteroscedasticity, and/or high variability: a logarithmic transformation is appropriate to re-establish normality (Feng et al., 2013; West, 2022). Transformation did indeed normalize most data and thus, parametric tests were applied to these for morphological analysis. The myotube area data across all time-points did not normalize by classical log-transformation, and the structure of the experiment was not fully compatible with the non-parametric Friedman's ANOVA assumptions. Which demands a balanced design with equal observations for each combination of time-point and condition. To balance the data frame, the means of each combination were calculated and assigned as an observation and thereby enabling Friedman's ANOVA to work. A pairwise Nemenyi Test was conducted to compare individual conditions (Demšar, 2006; Pereira et al., 2015). Both Friedman's ANOVA and Nemenyi are derived from the PMCMRplus package (Version 1.9.6, 2022-08-16). Because of this prior transformation to suit Friedman's ANOVA, there is an argument that a Box-Cox transformation is equally, if not more, appropriate. A Box-Cox transformation use a power parameter, lambda ( $\lambda$ ), to determine the type of transformation used (i.e., what power to raise data in), which maximize the log-likelihood of the data and is therefore considered the most optimal value for transforming the data (Box & Cox, 1982; Yeo & Johnson, 2000).

$$y(\lambda) = \begin{cases} \frac{y^\lambda - 1}{\lambda}, & \text{if } \lambda \neq 0 \\ \log(y), & \text{if } \lambda = 0 \end{cases}$$

**Equation 2:** *The Box-Cox transformation based on the value of lambda ( $\lambda$ ). If  $\lambda = 0$ , a standard log-transformation is used. If, however,  $\lambda \neq 0$ , then the box-cox transformation is used with  $\lambda$  as the power parameter.*

$\lambda$  was calculated within the MASS package for R (version 7.3-60, 2023-05-04), and estimated to be  $\sim -0.5$ . Thus, reducing the equation above to:  $y^{-0.5} = 1/(\sqrt{y})$ ; (Box & Cox, 1982). This normalized the data and enabled the use of parametric models.



Based on the experiment design, a mixed-effects ANOVA with crossed random effects is appropriate. The crossed random effects account for the variability between the experiment runs (ID), whilst the fixed effects capture the effects of the conditions (CT, ET, LTA, LT, MA, and ME) and time (3D, 7D, and 10D). Herein the conditions LTA and LT, and MA and ME (see Figure 2.) are pooled together to LATE and MEM for all morphological analysis of myotube diameter as these were morphologically identical. A post hoc TukeyHSD adjusted pairwise test was used when comparing conditions. The estimated marginal means (emmeans) package for R (version 1.8.6, 2023-05-11), was used to run a custom contrast analysis to investigate memory effects in the ME condition. Herein two contrast models were designed: (i) ME vs (ET + LATE)/2 and (ii) (ME – LT) vs (LT – CT), specifically for the 7- to 10-day time-points.

To further support the conclusions of these statistical models, non-parametric tests were also applied to all non-transformed data, whereby a Kruskal-Wallis and Dunn's pairwise tests were used for individual time-points. Alternative to the mixed effects model, a Friedman's ANOVA and Dunn's test and Mann-Whitney post hoc pairwise tests. The results of the non-parametric tests are in concordance with the parametric, therefore, the parametric tests remain presented herein for simplicity.

## Part IV – Results and Discussion

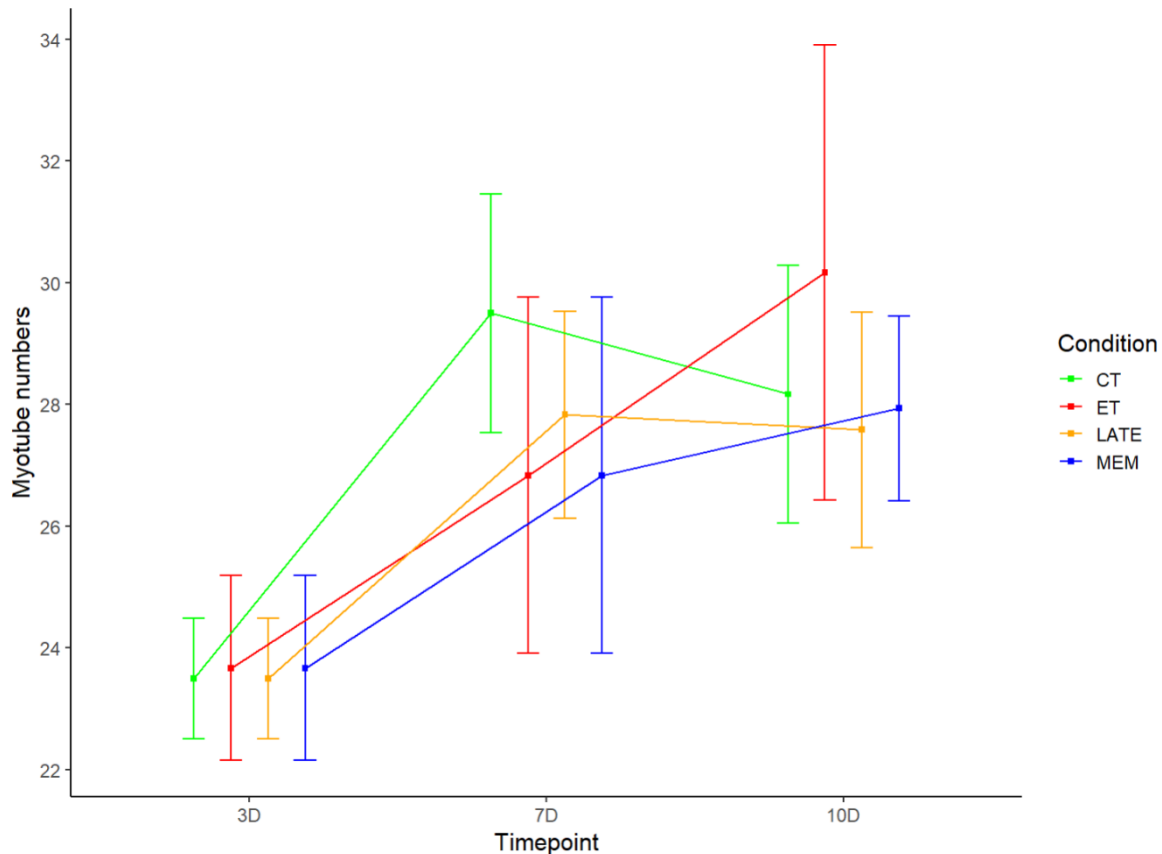
### 4.0 Results

#### 4.0.1 Morphological analysis

For morphological analysis of myotube diameter, the conditions LTA and LT, and MA and ME, are pooled into LATE and MEM, respectively. Because of the exclusion of myobranches when collecting diameter data, these conditions differed marginally on any measure with little variance between them. Thus, they are pooled for simplicity. Moreover, the pooling had no effect on any statistical model for myotube diameter. For myotube area this was reversed due as the individual conditions differed significantly. Additionally, due to the large SD figures are presented with SE to avoid warping.

#### 4.0.1.1 Myotube number

Analysis of myotube numbers at individual time-points (3D, 7D, and 10D) revealed no significant difference between conditions (CT, ET, LATE, and MEM); ( $P > 0.05$ ). Similarly, when considering all time-points, the mixed effects model found no difference among any conditions ( $P = 0.93$ ). Mean  $\pm$  SD myotube numbers for all time-points were CT:  $27.1 \pm 4.8$ , ET:  $26.9 \pm 7.2$ , LATE:  $26.6 \pm 5.5$ , and MEM:  $26.7 \pm 5.8$ . Mean change in myotube numbers from 3- to 10-days was CT:  $4.7 \pm 2.76$ , ET:  $6.5 \pm 5.45$ , LATE:  $4.1 \pm 4.28$ , MEM:  $4.2 \pm 2.15$ . These findings indicate that myotube numbers did not show any difference between conditions examined, nor over time, suggesting that testosterone, nor culture time, had a significant effect on myotube formation. However, limitations in sample size impose a substantial caveat to this interpretation. As seen in figure 3, there is a trend for an increase in myotubes over time, but no indication of treatment effects.



**Figure 3** Illustrating myotube numbers over time  $\pm$  SE. The observations are all non-significant albeit showing a tendency for increased myotubes over time.

#### 4.0.1.2 Myotube diameter

Myotube diameter at the 3-day time-point was  $25.4 \pm 9.9 \mu\text{m}$  for CT, and  $26.4 \pm 9.4 \mu\text{m}$  for ET, with no significant difference between the two ( $P = 0.08$ ). Myotube images are found in figure 4. Myotube diameter values are summarized in Table 2 and illustrated in figure 5.

At 7-days, CT had a mean diameter of  $25 \pm 9.5 \mu\text{m}$ , ET  $27.5 \pm 9.4 \mu\text{m}$ , and LATE  $24.8 \pm 9.1 \mu\text{m}$  (figure 5). ET was significantly larger than the CT and LATE conditions ( $P < 0.01$ ). Whereas CT and LATE were not significantly different ( $P = 0.99$ ), which is as expected due to LATE being exposed to testosterone for only 4 hours before imaging.

At 10-days, the CT condition had a mean diameter of  $25.5 \pm 9.5 \mu\text{m}$ , with ET at  $30.3 \pm 10.8 \mu\text{m}$ , LATE at  $30.1 \pm 12.3 \mu\text{m}$ , and MEM with  $32.6 \pm 13.8 \mu\text{m}$  (figure 5). Here there was a significantly larger mean myotube diameter in all testosterone conditions (i.e., ET, LATE and MEM) compared with CT condition ( $P < 0.01$ ). However, there was no difference between the ET and LATE condition ( $P = 0.78$ ). Suggesting that testosterone was effective for inducing increased diameter, however, their respective exposure did not cause a difference in their diameter morphology despite happening at different stages of growth. Interestingly, the MEM condition was significantly larger than both ET and LATE ( $P < 0.01$ ), suggesting that the addition of a second treatment was sufficient to evoke a difference from a singular treatment.

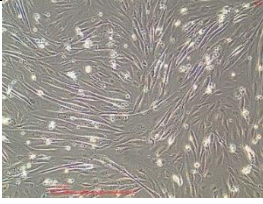
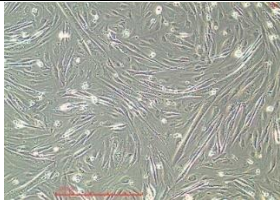
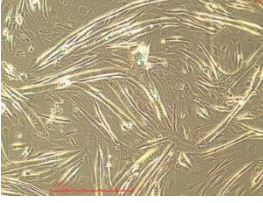
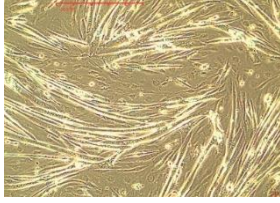
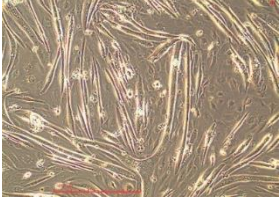
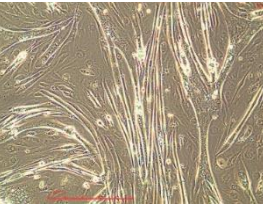

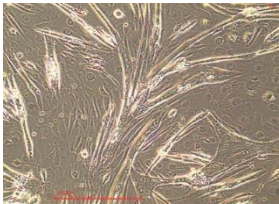
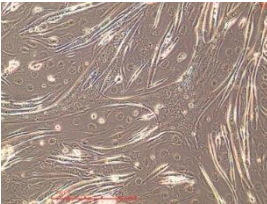
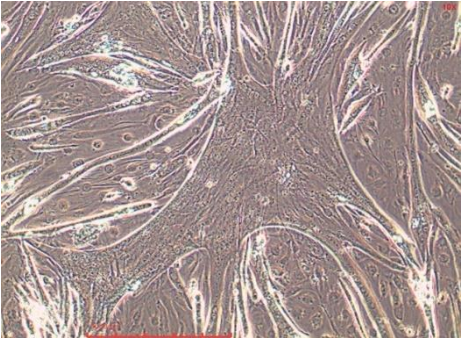
To investigate further, the mixed effects model including all time-points revealed significant effects of the conditions ( $P < 0.01$ ) and time-point ( $P < 0.01$ ) on myotube diameter, indicating that myotubes vary across different treatments and time-points (see figure 5). The pairwise comparisons revealed that the change from 3- to 10-days for all treatment conditions (ET, LATE, and MEM) were significantly greater than for CT ( $P < 0.01$ ). ET and LATE were no different from each other ( $P = 0.064$ ), which is expected as these are exposed to the same treatment albeit at different time-points. Interestingly, MEM was significantly different from both LATE and ET ( $P = 0.04$ ). The change from 7- to 10-days corroborate these findings further with all testosterone conditions significantly larger than CT ( $P < 0.01$ ), with ET and LATE not significantly different ( $P = 0.064$ ), and with MEM being significantly larger than both LATE ( $P < 0.01$ ) and ET ( $P < 0.01$ ). A custom contrast analysis compared MEM with the combined effects of ET and LATE,

which showed no difference ( $P = 0.18$ ), and another comparing the magnitude of change from 7D to 10D between MEM and LATE, which was significant ( $P = 0.032$ ). Albeit contradictory, this suggesting that there could be a memory effect of repeated treatment of testosterone on myotube diameter.

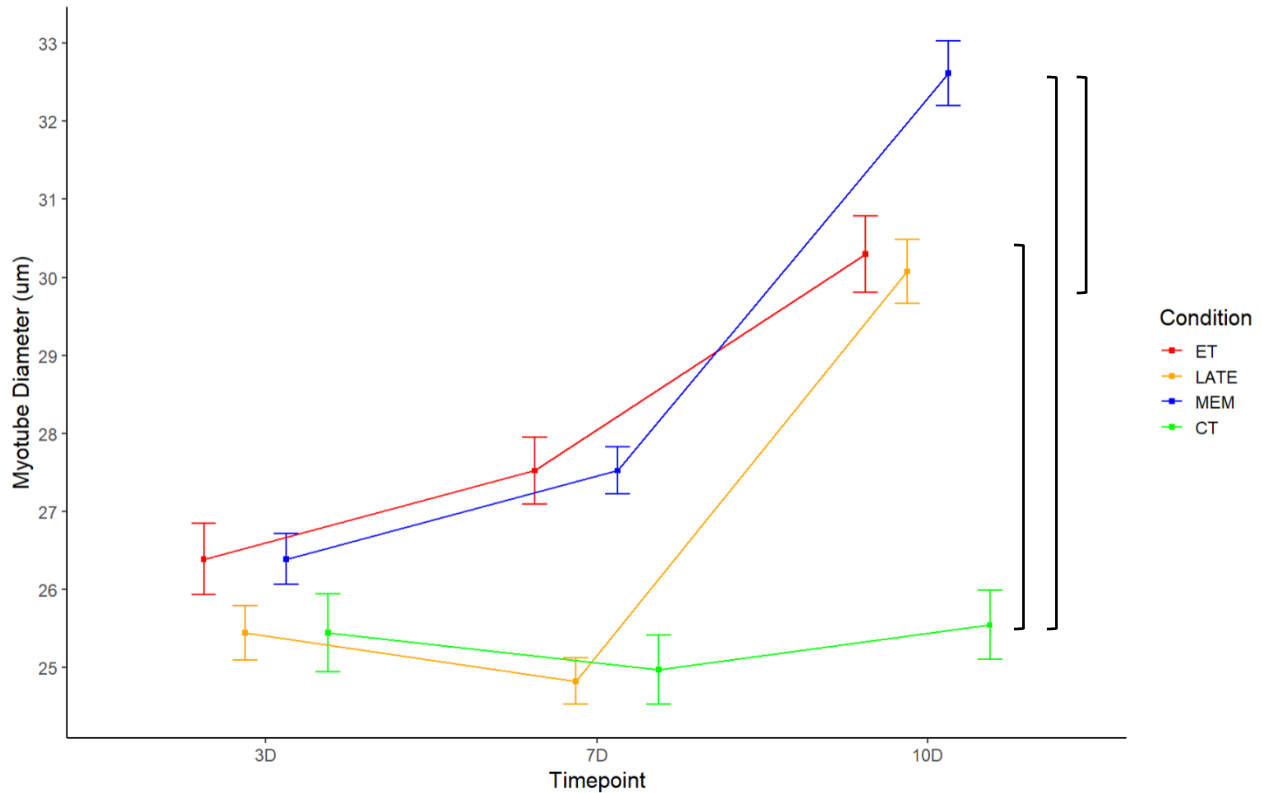
Interestingly, CT and LATE did not change significantly from 3- to 7-days ( $P = 0.49$  and  $P = 0.37$ , respectively), contrary to ET which did ( $P < 0.01$ ), which posits either that the diameter morphology of these cells was fully matured by 3 days or the indication of high variability. It could also be a measurement error due to the exclusion of myobranched for diameter measurements, possibly creating an artifact (see figure 4B).

Table 2. Myotube Diameter Summary Statistics

condition	timepoint	Mean	SD	Min	Max
CT	3D	25.45	9.90	8.04	58.24
CT	7D	24.97	9.48	6.38	67.31
CT	10D	25.54	9.30	8.07	80.32
ET	3D	26.39	9.33	7.41	72.25
ET	7D	27.52	9.41	9.20	76.10
ET	10D	30.30	10.78	6.50	68.51
LATE	3D	25.45	9.90	8.04	58.24
LATE	7D	24.83	9.11	7.44	75.00
LATE	10D	30.08	12.30	6.50	101.57
MEM	3D	26.39	9.33	7.41	72.25
MEM	7D	27.52	9.41	9.20	76.10
MEM	10D	32.62	13.84	7.76	153.49

A	CT	ET	LATE	MEM
3 days				
7 days				
10 days				
<b>B</b>	 <span data-bbox="781 1014 971 1045">MEM 10-days</span>			

**Figure 4** Representative example-images used in the morphological analysis. **A:** Shows representative images across time-points for each condition. **B:** Show an example image of the Myobranches to illustrate their enlarged size compared to normal myotubes. The scale-bar indicates 1000  $\mu\text{m}$ , and all images are magnified 10X.



**Figure 5.** Illustrate the change in mean Myotube Diameter ( $\mu\text{m}$ ) over time  $\pm$  SE. Here we observe the memory condition being significantly larger than both CT and LATE ( $P < 0.01$ ). We also see that the untreated conditions do not change significantly over the course of the experiment.

#### 4.0.1.3 Myotube area

At the 3-day timepoint the mean myotube area for CT was  $15,710 \pm 11,094 \mu\text{m}^2$ , and for ET  $15,903 \pm 11,841 \mu\text{m}^2$ . With no difference between conditions ( $P = 0.67$ ). Myotube images are found in figure 4A. Myotube area values are summarized in Table 3A and figure 6A.

At 7-days the mean area for CT  $24,958 \pm 26,154 \mu\text{m}^2$ , ET  $27,046 \pm 15,539 \mu\text{m}^2$ , and LTA  $26,072 \pm 21,571 \mu\text{m}^2$ . The pairwise comparisons at this time-point showed ET to be significantly larger than CT ( $P < 0.01$ ), whilst CT and LTA were not significantly different ( $P = 0.10$ ), as suspected due to LTA being exposed to testosterone for only 4 hours prior to imaging. However, for ET and LTA there was also no significance ( $P = 0.08$ ). Posing a contradiction.

At 10-days the CT condition reached a mean area of  $34,475 \pm 51,506 \mu\text{m}^2$ , ET  $34,057 \pm 49,096 \mu\text{m}^2$ , LT  $37,791 \pm 45,855 \mu\text{m}^2$ , LTA  $34,930 \pm 51,694 \mu\text{m}^2$ , MA  $34,869 \pm 40,021 \mu\text{m}^2$ , and ME  $46,367 \pm 97,481 \mu\text{m}^2$ . At this time-point ME was significantly larger than all other conditions ( $P$



< 0.01). Whereas the single treated conditions were no different from control ( $P > 0.05$ ); figure 6A and table 3A.

The mixed effects model across all time-points revealed significant effects of the conditions ( $P < 0.01$ ) and time ( $P < 0.01$ ) on myotube area, indicating that myotubes vary across different treatments and time-points (figure 6A). Indeed, untreated CT increased significantly from 3- to 10-days (from  $15,710 \pm 11,094$  to  $34,475 \pm 51,505 \mu\text{m}^2$ ;  $P < 0.01$ ). Interestingly, the change in ET ( $18,153 \pm 37,255 \mu\text{m}^2$ ) from 3- to 10-days was not different from CT ( $P > 0.05$ ); (figure 6A). Conversely, from 3- to 7-days ET grew significantly larger than CT (ET:  $11,142 \pm 3,699$  vs CT:  $9,248 \pm 15,059 \mu\text{m}^2$ ;  $P < 0.01$ ). Suggesting, that the ET treatment provided augmented hypertrophy immediately after exposure but that this effect was abolished and eventually plateaued by day 10. Interestingly, CT grew significantly more than ET from 7- to 10-days (ET:  $7,011 \pm 33,556$  vs CT:  $9,517 \pm 25,352 \mu\text{m}^2$ ;  $P < 0.01$ ), resulting in them having no difference at 10-days ( $P > 0.05$ ). Moreover, the pairwise comparisons revealed that the change from 3- to 10-days for LT ( $22,081 \pm 34,761 \mu\text{m}^2$ ) and ME ( $30,464 \pm 85,640 \mu\text{m}^2$ ) were significantly greater than for CT ( $18,765 \pm 40,411 \mu\text{m}^2$ ;  $P < 0.01$ ), ET ( $18,153 \pm 37,255 \mu\text{m}^2$ ;  $P < 0.01$ ), and from each other ( $P < 0.01$ ). However, LTA did not differ from control at any time-point ( $P > 0.05$ ). A custom contrast to compare ME with the combined effects of ET and LT, and another comparing the magnitude of change from 7- to 10-days between ME and LT, revealed significant differences in both ( $P < 0.01$ ). Suggesting a memory effect in the ME condition, whereby the repeated treatment of testosterone enabled more hypertrophy than the single treatment in LT at the same time-point. Conversely, MA exhibited no significant difference from CT, ET, or LTA from 7- to 10-days ( $P > 0.05$ ). Moreover, growing less than LT in this timespan (MA:  $7,823 \pm 24,482$  vs LT:  $11,719 \pm 24,284 \mu\text{m}^2$ ;  $P < 0.01$ ). Indicating that this effect relies on the presence of testosterone in media for longer than 4-hours.

#### 4.0.1.4. Myobranche area

The myobranches observed in our cells resulted in a much broader spread in the data as observed by the large SDs and effects on myotube area when excluded (figure 6B). Due to these posing a large effect on the analysis, a mixed effects model on myobranches alone was performed. This revealed that ME ( $289,954 \pm 224,394 \mu\text{m}^2$ ) either reached or approached statistical significance compared to all other conditions. Whereby: ME – CT ( $P = 0.035$ ), ME – ET ( $P = 0.055$ ), ME – LT

( $P = 0.09$ ), ME – LTA ( $P = 0.03$ ), ME – MA ( $P = 0.08$ ); see table 4 for means and SD. In comparison, MA was not significantly different from any condition ( $P > 0.05$ ); (table 4 and figure 7B). The contrast analysis had insufficient power to output meaningful data due to missing values because of the small sample size. However, these results indicate that the repeated exposure and incubation with testosterone from 7- to 10-days, was enough to elicit a much larger effect on Myobranche area compared with the 4-hour repeated treatment.

Excluding the myobranche from the dataset resulted in a significant difference in results. The CT condition grew significantly from 3- to 7-days ( $P < 0.01$ ) and remained unchanged from 7- to 10-days. The ET condition grew significantly larger than both CT and LATE from 3- to 7-days ( $P < 0.01$ ). Interestingly, this was reversed from 7- to 10- days, whereby the ET condition decreased in size and was no different from either CT or LATE at 10-days ( $P < 0.01$ ). Additionally, the LATE condition followed a similar trend, growing significantly from 3- to 7-days, becoming surprisingly larger than CT at 7-days ( $P < 0.01$ ), albeit less than ET ( $P < 0.01$ ), and remaining unchanged from 7- to 10- days despite testosterone treatment. The MEM condition followed the same trend by increasing significantly from 3- to 7-days ( $P < 0.01$ ), and more so than CT ( $P < 0.01$ ). Then decreasing from 7- to 10-days ( $P < 0.01$ ). At 10-days there was no difference between any conditions. Overall, these results suggest that from 3- to 7- days most myotubes grew independently, whereby testosterone treatment had a significant effect compared to control. From 7- to 10-days these effects were no longer occurring in classical myotubes and likely occurring within the myobranche themselves as seen in figures 7. Myotube area data with myobranche excluded is found in table 3B and figure 6B.



**Table 3A. Myotube Area Summary Statistics**

condition	timepoint	Mean	SD	Min	Max
CT	3D	15710.07	11094.18	3889.87	61402.15
CT	7D	24958.49	26153.95	4029.82	188907.05
CT	10D	34475.29	51505.77	3750.80	421867.03
ET	3D	15903.23	11840.72	4155.27	91011.92
ET	7D	27045.84	15539.49	7166.77	104878.83
ET	10D	34056.64	49095.84	5624.20	405082.11
LT	3D	15710.07	11094.18	3889.87	61402.15
LT	7D	26071.94	21570.93	5600.29	155444.83
LT	10D	37790.65	45855.48	4998.41	293490.91
LTA	3D	15710.07	11094.18	3889.87	61402.15
LTA	7D	26071.94	21570.93	5600.29	155444.83
LTA	10D	34930.16	51694.35	5317.28	435917.57
MA	3D	15903.23	11840.72	4155.27	91011.92
MA	7D	27045.84	15539.49	7166.77	104878.83
MA	10D	34868.77	40020.82	3918.21	266011.64
ME	3D	15903.23	11840.72	4155.27	91011.92
ME	7D	27045.84	15539.49	7166.77	104878.83
ME	10D	46367.13	97481.33	5181.76	843598.53

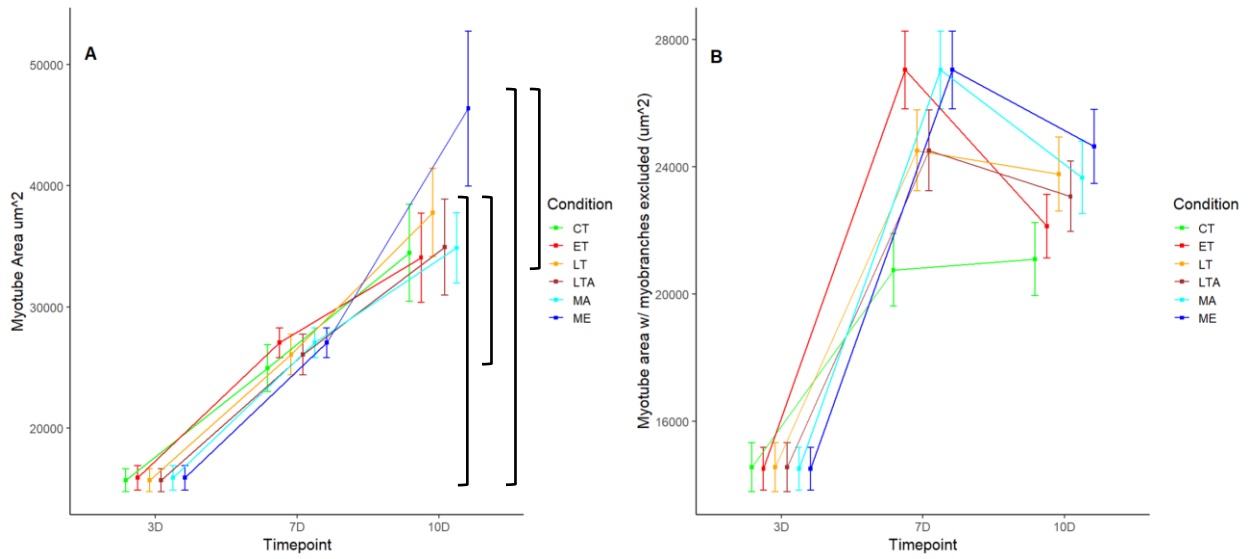
**Table 3B. Myotube Area w/ myobranched excluded**

condition	timepoint	Mean	SD	Min	Max
CT	3D	14566.87	8947.40	3889.87	45945.65
CT	7D	20760.81	14997.93	4029.82	89779.97
CT	10D	21101.99	13863.17	3750.80	66003.67
ET	3D	14507.54	7851.61	4155.27	39334.45
ET	7D	27045.84	15539.49	7166.77	104878.83
ET	10D	22136.40	12587.51	5624.20	75765.31
LT	3D	14566.87	8947.40	3889.87	45945.65
LT	7D	24510.55	16314.60	5600.29	92071.91
LT	10D	23768.56	13750.92	4998.41	67641.90
LTA	3D	14566.87	8947.40	3889.87	45945.65
LTA	7D	24510.55	16314.60	5600.29	92071.91
LTA	10D	23070.97	13775.24	5317.28	70866.55
MA	3D	14507.54	7851.61	4155.27	39334.45
MA	7D	27045.84	15539.49	7166.77	104878.83
MA	10D	23662.75	14824.43	3918.21	84665.98
ME	3D	14507.54	7851.61	4155.27	39334.45
ME	7D	27045.84	15539.49	7166.77	104878.83
ME	10D	24638.76	16940.96	5181.76	103930.17

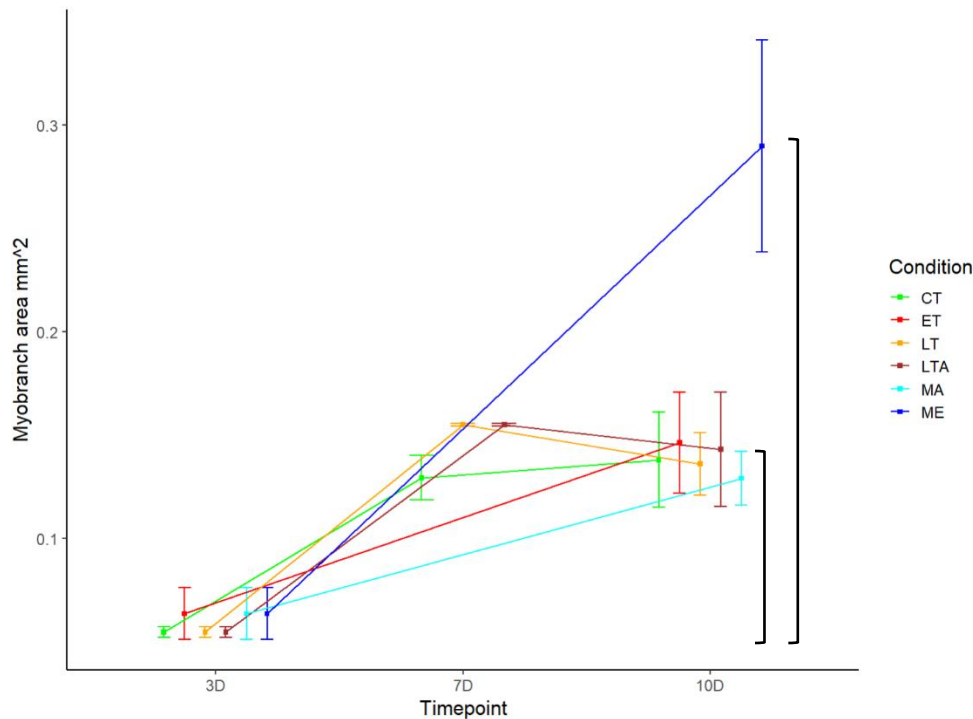
**Table 4. Myobranched Area summary statistics**

condition	timepoint	Mean	SD	Min	Max
CT	3D	54579.03	5155.58	50469.31	61402.15
CT	7D	129300.86	28675.46	107389.99	188907.05
CT	10D	137942.36	99990.70	47361.29	421867.03
ET	3D	63356.99	25122.13	37924.27	91011.92
ET	10D	146247.09	100725.28	55719.87	405082.11
LT	3D	54579.03	5155.58	50469.31	61402.15
LT	7D	154886.80	789.18	154328.76	155444.83
LT	10D	135945.27	67992.55	54037.79	293490.91

condition	timepoint	Mean	SD	Min	Max
LTA	3D	54579.03	5155.58	50469.31	61402.15
LTA	7D	154886.80	789.18	154328.76	155444.83
LTA	10D	143058.08	113793.77	50924.74	435917.57
MA	3D	63356.99	25122.13	37924.27	91011.92
MA	10D	128999.32	58265.84	58262.91	266011.64
ME	3D	63356.99	25122.13	37924.27	91011.92
ME	10D	289953.68	224393.51	63456.63	843598.53



**Figure 6.** Mean change in Myotube Area ( $\mu\text{m}^2$ ) over time for all conditions  $\pm$  SE. **A:** Illustrate the myotube area with the myobranched data included. Herein ET grew significantly larger than CT from 3- to 7- days, which was plateaued and decreased to less than CT by day 10. LT grew significantly larger than CT, ET, LTA, and MA from 7-to 10-days ( $P < 0.01$ ). ME grew significantly larger than all other conditions at all time-points ( $P < 0.01$ ), with the magnitude of change from 7- to 10-days being significantly larger than LT ( $P < 0.01$ ). **B:** Illustrate the effects of removing the myobranched area data from the analysis, and show how the later stages of growth likely lead to increasingly larger myobranched.



**Figure 7.** Mean myobranched area analysis over time for all conditions  $\pm$  SE. Illustrate the myobranched area alone for all individual conditions highlighting that the ME condition differs significantly from nearly all other conditions, and that all conditions changed significantly from 3- to 10-days ( $P < 0.01$ ).

#### 4.1.0 Gene expression analysis

For all gene expression analysis, LATE and MEM is separated into their respective conditions (LTA and LT, and MA and ME). This is done due to the mRNA response being more acute than the morphological, and because their respective values have a greater variance between them.

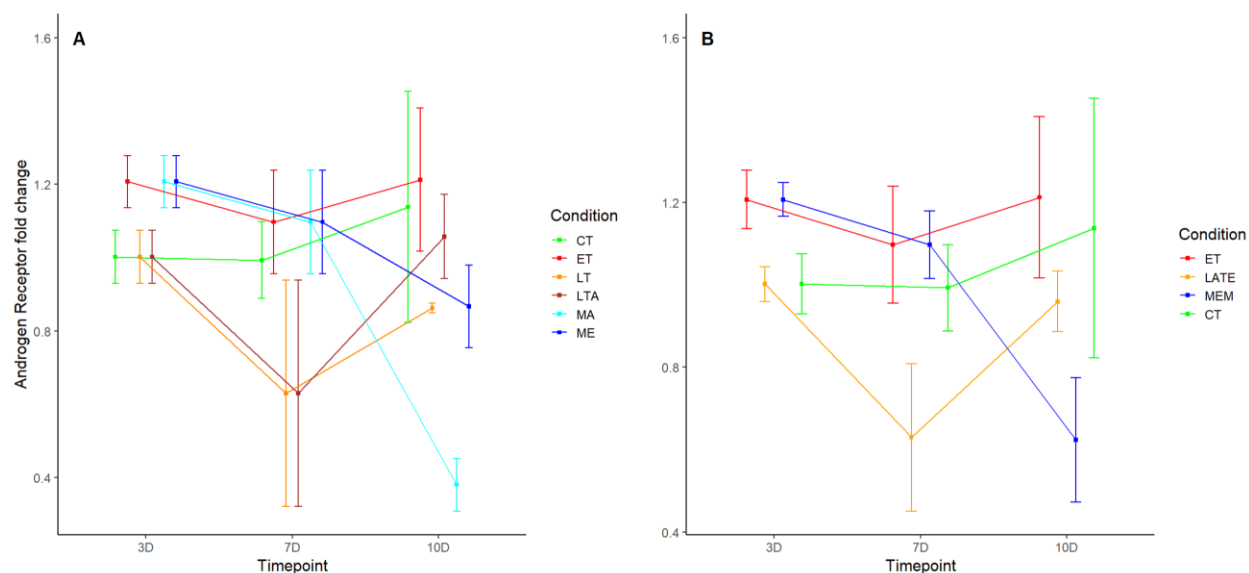
##### 4.1.1 Androgen Receptor

There is a significant main effect for condition ( $P < 0.01$ ), but not for time-point ( $P > 0.05$ ). However, there was a near significance for an interaction effect between the technical replicates ( $P = 0.08$ ), suggesting high variance across the experimental runs. Post-hoc pairwise comparisons yielded no significant difference between any condition ( $P > 0.05$ ), apart from MA vs CT nearly reaching significance ( $P = 0.053$ ). The fold change across conditions and time is summarized in table 4. and illustrated in figure 8A. Overall, there seems to be no effect of one dose of testosterone on AR mRNA-levels, with the repeated dosing causing a decreased gene expression in the memory conditions (MA and a trend for ME); (Figure 8A and 13A).

If, however, the calibrator is set to be the control condition at the 0-hour time-point. There is a trend for downregulated gene expression of AR across all conditions and time-points compared to 0-hour control. Whereby the mean fold change of all conditions from 3- to 10-days is  $\sim 0.51 \pm 0.10$  compared with CT at 0-hours ( $P = 0.078$ ). The near-significant difference between MA and CT remains ( $P = 0.053$ ). This suggest that there is a trend for downregulated AR gene expression when moving from the proliferative cell cycle stages and into the terminally differentiated G0-state, whereby repeated dosing of testosterone possibly augments this effect (Figure 8A and 8B).

**Table 5. Androgen Receptor fold change summary**

condition	timepoint	Mean	SD	Min	Max	condition	timepoint	Mean	SD	Min	Max
CT	3D	1.00	0.10	0.93	1.07	LTA	3D	1.00	0.10	0.93	1.07
CT	7D	0.99	0.15	0.89	1.10	LTA	7D	0.63	0.44	0.32	0.94
CT	10D	1.14	0.45	0.82	1.45	LTA	10D	1.06	0.16	0.94	1.17
ET	3D	1.21	0.10	1.14	1.28	MA	3D	1.21	0.10	1.14	1.28
ET	7D	1.10	0.20	0.96	1.24	MA	7D	1.10	0.20	0.96	1.24
ET	10D	1.21	0.28	1.02	1.41	MA	10D	0.38	0.10	0.31	0.45
LT	3D	1.00	0.10	0.93	1.07	ME	3D	1.21	0.10	1.14	1.28
LT	7D	0.63	0.44	0.32	0.94	ME	7D	1.10	0.20	0.96	1.24
LT	10D	0.86	0.02	0.85	0.88	ME	10D	0.87	0.16	0.75	0.98

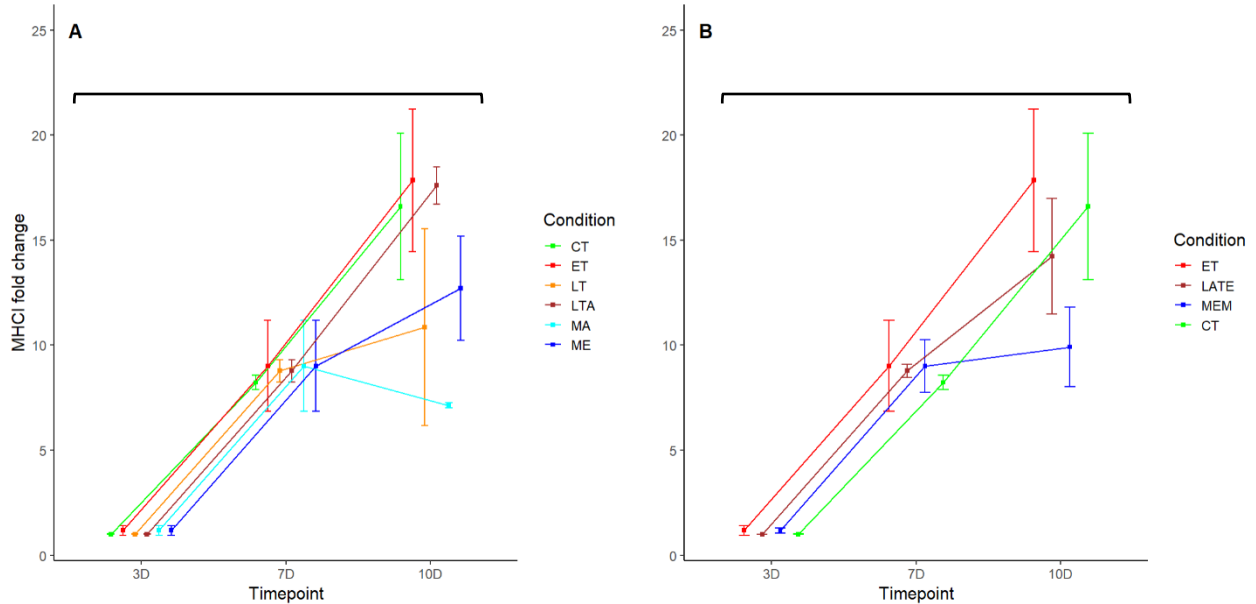


#### 4.1.2. MHCI – Myosin heavy chain IId/Ix

There is a significant main effect of time-point ( $P = 0.02$ ), indicating that the gene expression was different across time. The main effect of condition, however, was not significant ( $P > 0.05$ ), suggesting no difference between the conditions and no effect of testosterone on MHCI expression. Interestingly, however, there was a substantial increase in gene expression for all conditions. Compared with the 3-day control calibrator, the mean fold change at 7-days was  $29 \pm 1.2$ , and  $58.6 \pm 4.76$  at the 10-day time-point. Compared with the 0-hour control calibrator (i.e. proliferating cells): a mean fold change of  $33.5 \pm 5.13$  at the 3-day time-point,  $264.8 \pm 54.65$  at the 7-day time-point, and  $450.12 \pm 146.25$  at the 10-day time-point. These results indicate that the expression of myosin heavy chain IId/x is substantially and significantly increased over time compared with either baseline calibration, with no effect from the treatment of testosterone (figure 9A). These effects were consistent irrespective of condition pooling (figure 9B). Mean fold change compared with the 3-day calibrator is found in table 5. and illustrated in figures 9A, 9B, and 13B.

**Table 6. MHCI fold change summary**

condition	timepoint	Mean	SD	Min	Max	condition	timepoint	Mean	SD	Min	Max
CT	3D	1.00	0.02	0.99	1.01	LTA	3D	1.00	0.02	0.99	1.01
CT	7D	8.22	0.48	7.88	8.57	LTA	7D	8.78	0.75	8.25	9.31
CT	10D	16.61	4.93	13.12	20.09	LTA	10D	17.61	1.25	16.72	18.49
ET	3D	1.18	0.32	0.96	1.40	MA	3D	1.18	0.32	0.96	1.40
ET	7D	9.01	3.07	6.84	11.19	MA	7D	9.01	3.07	6.84	11.19
ET	10D	17.85	4.80	14.46	21.24	MA	10D	7.13	0.17	7.01	7.25
LT	3D	1.00	0.02	0.99	1.01	ME	3D	1.18	0.32	0.96	1.40
LT	7D	8.78	0.75	8.25	9.31	ME	7D	9.01	3.07	6.84	11.19
LT	10D	10.86	6.64	6.16	15.55	ME	10D	12.70	3.50	10.22	15.18



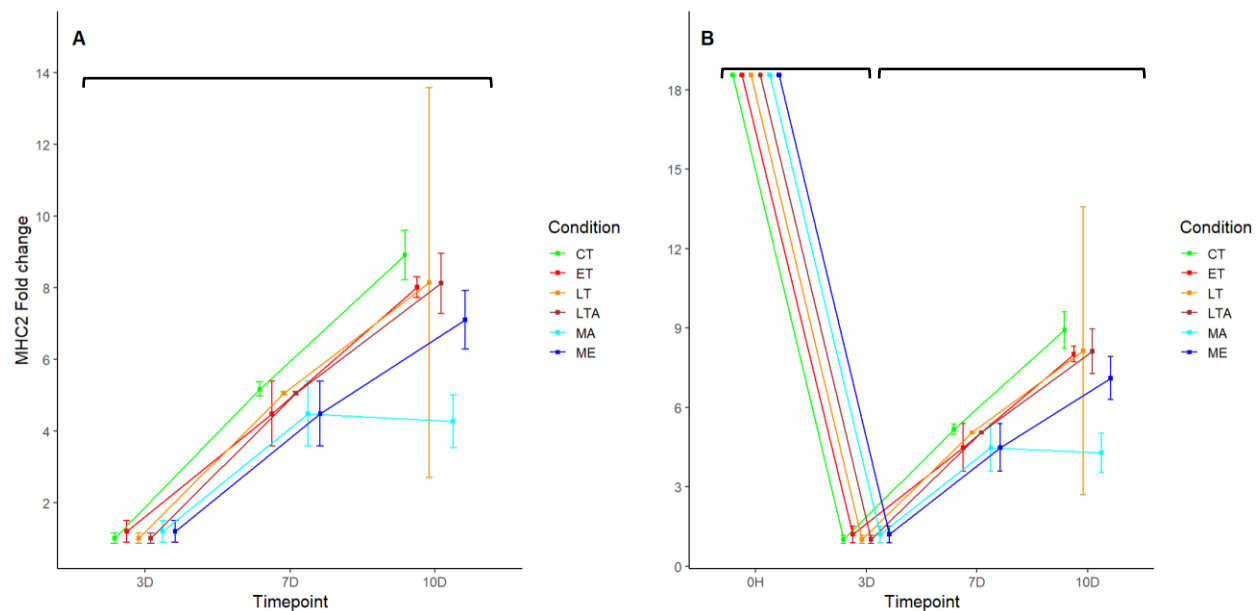
**Figure 9. MHC1:** Illustrating the mean fold change  $\pm$  SE across time. **A:** Plots the fold change for all individual conditions. Here we can see a trend for the acutely dosed conditions LTA and MA (4-hours at 7-days) deviating from the overall pattern. **B:** Plots the fold change for the pooled conditions. Altering the calibration to 0-hour would only increase the magnitude of change and not the directionality. All conditions change significantly with time ( $P < 0.01$ ), without pairwise differences.

#### 4.1.3 MHC2 – Myosin heavy chain IIa

There was a significant effect for time ( $P = 0.02$ ), indicating a difference in gene expression between the time-points. There was no significant main effect of condition and zero pairwise difference to be found between conditions ( $P > 0.05$ ). There was a substantial increase in gene expression over time with progressively increased gene expression from 3- to 10-days. Compared with the 3-day control calibrator, the mean fold change for all conditions at 7-days was  $4.8 \pm 1.9$ , and  $7.68 \pm 1.93$  at 10-days. Whereas when compared with the 0-hour calibrator, the gene expression was reduced significantly ( $P = 0.02$ ), with a mean fold change of  $0.05 \pm 0.01$  at 3-days,  $0.26 \pm 0.04$  at 7-days, and  $0.3 \pm 0.1$  at 10-days. These results indicate that MHC2 gene expression is significantly reduced (by about 95%) when the cell terminally differentiates, with a progressive and significant increase in expression from 3- to 10-days (up to ~9-fold) without any effect from the treatment of testosterone. Mean fold change is summarized in table 6. and illustrated in figure 9A, 9B, and 12C.

**Table 7. MHC2 fold change summary**

condition	timepoint	Mean	SD	Min	Max	condition	timepoint	Mean	SD	Min	Max
CT	3D	1.01	0.20	0.87	1.15	LTA	3D	1.01	0.20	0.87	1.15
CT	7D	5.17	0.28	4.97	5.37	LTA	7D	5.05	0.06	5.01	5.09
CT	10D	8.91	0.98	8.22	9.60	LTA	10D	8.12	1.19	7.28	8.96
ET	3D	1.19	0.44	0.89	1.50	MA	3D	1.19	0.44	0.89	1.50
ET	7D	4.48	1.28	3.58	5.38	MA	7D	4.48	1.28	3.58	5.38
ET	10D	8.01	0.41	7.72	8.30	MA	10D	4.27	1.04	3.54	5.01
LT	3D	1.01	0.20	0.87	1.15	ME	3D	1.19	0.44	0.89	1.50
LT	7D	5.05	0.06	5.01	5.09	ME	7D	4.48	1.28	3.58	5.38
LT	10D	8.14	7.69	2.70	13.58	ME	10D	7.10	1.14	6.29	7.91



**Figure 10. MHC2:** Illustrating the mean fold change  $\pm$  SE across time. **A:** Plots all individual conditions and illustrate how the MA condition trends non-significantly differently to all other conditions. This also shows how the small sample size is subject to large variations as the LT condition has two observations on either end of the figure. **B:** Shows the substantial and significant ( $P < 0.01$ ) reduction in gene expression from cell cycle to G0 (0H to 3D), with the progressive increase in gene expression from 3- to 10-days. The only significant effect is this increase over time for all conditions ( $P < 0.01$ ).

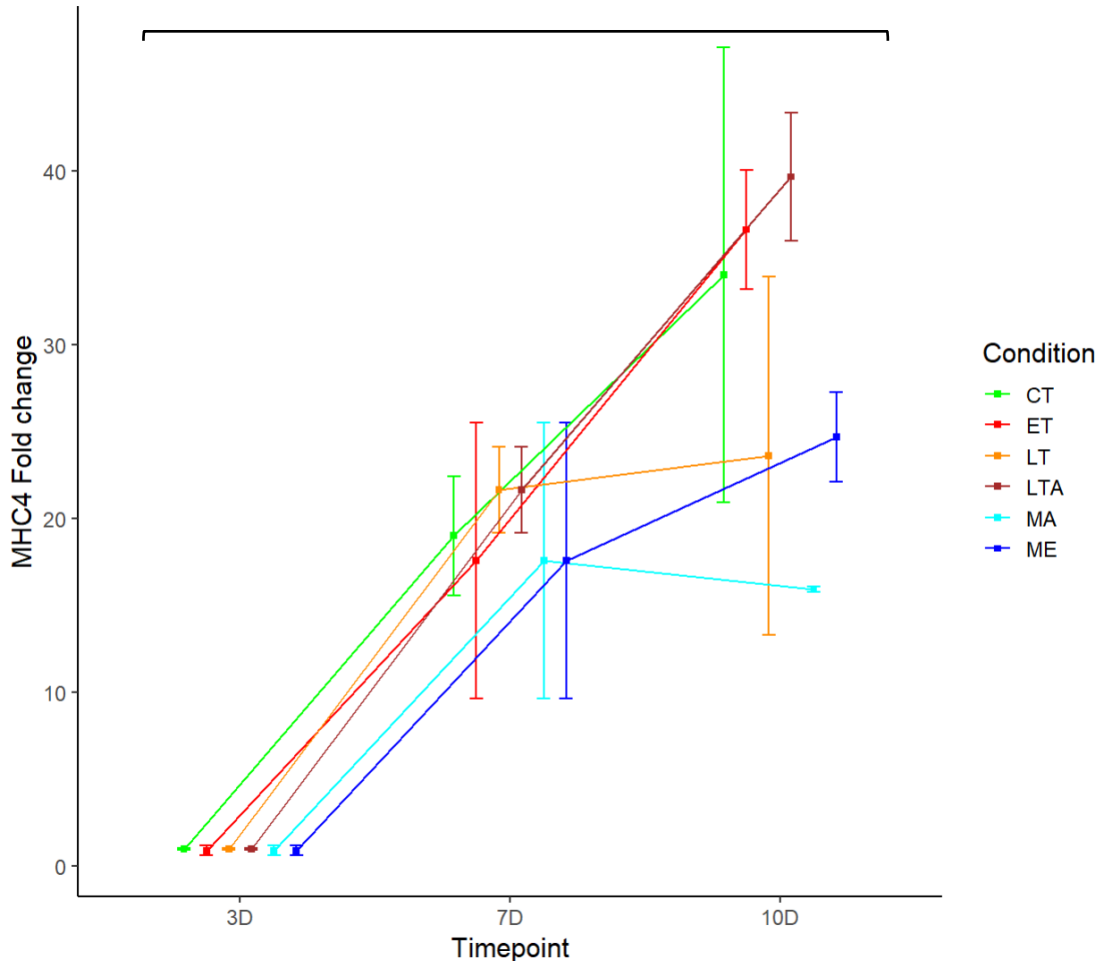
#### 4.1.4 MHC4 – Myosin heavy chain IIb

There was a near-significant effect for time ( $P = 0.054$ ), indicating a difference by progressively increased gene expression between the time-points. There was no significant effect of condition nor a pairwise difference to be found ( $P > 0.05$ ). There was a substantial increase in gene expression over time from ~1-fold the calibrator (CT at 3-days) and to a mean of  $29.09 \pm 7.83$ -fold change by 10 days. The mean and SD values of the fold change from the 3-day CT calibrator is found in [table 6](#), and illustrated in figure 11 and 13D. By changing the calibrator to 0-hour the directionality remained the same with the fold change increasing in magnitude. These results indicate that there is a substantial and significant increase in MHC4 gene expression from 0-hour and throughout all time-points to 10-days, without any observed effect of testosterone. There is, however, a non-significant trend for the memory conditions MA and ME to deviate from the overall trend from 7- to 10-days by a smaller fold change compared with all other conditions.

**Table 8. MHC4 fold change summary**

condition	timepoint	Mean	SD	Min	Max	condition	timepoint	Mean	SD	Min	Max
CT	3D	1.21	0.05	1.17	1.24	LTA	3D	1.21	0.05	1.17	1.24
CT	7D	22.96	5.84	18.83	27.10	LTA	7D	26.16	4.21	23.18	29.14
CT	10D	41.08	22.35	25.28	56.89	LTA	10D	47.88	6.32	43.41	52.35
ET	3D	1.09	0.49	0.74	1.43	MA	3D	1.09	0.49	0.74	1.43
ET	7D	21.24	13.53	11.67	30.80	MA	7D	21.24	13.53	11.67	30.80
ET	10D	44.21	5.83	40.09	48.34	MA	10D	19.23	0.28	19.03	19.43
LT	3D	1.21	0.05	1.17	1.24	ME	3D	1.09	0.49	0.74	1.43
LT	7D	26.16	4.21	23.18	29.14	ME	7D	21.24	13.53	11.67	30.80
LT	10D	28.49	17.59	16.06	40.93	ME	10D	29.81	4.37	26.72	32.90





**Figure 11. MHC4:** Illustrate the mean fold change  $\pm$  SE over time. Here the memory conditions trend non-significantly toward a deviation from the pattern by a lesser increase in gene expression, whereby the MA condition decrease from 7- to 10-days. The only significant effect is the increase in gene expression over time ( $P < 0.01$ ).

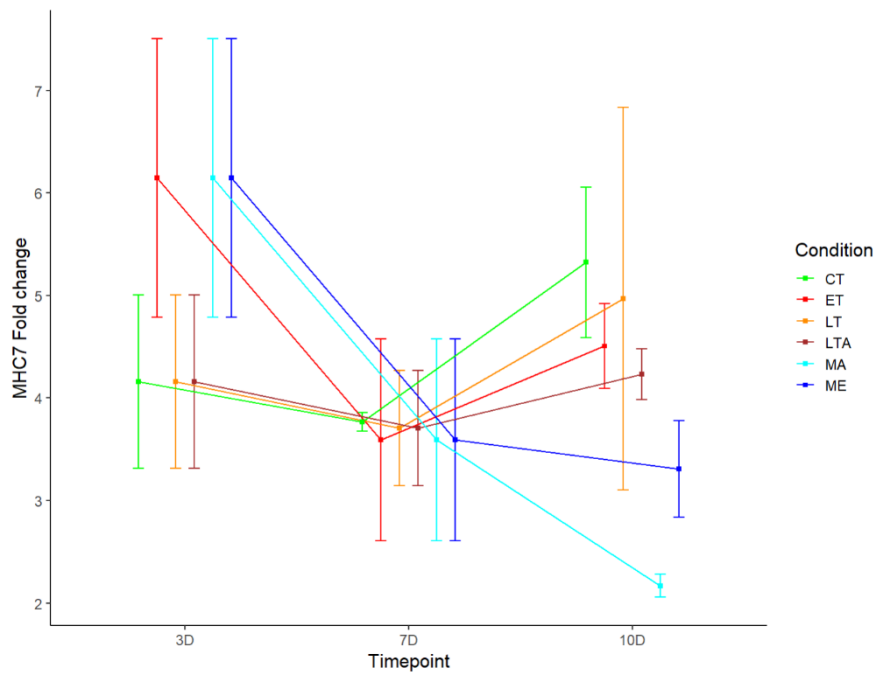
#### 4.1.5 MHC7 - Myosin heavy chain I

There were no significant effects for neither condition nor time-point ( $P > 0.05$ ), indicating that the expression of MHC7 remained unchanged from 3- to 10-days without any effect of testosterone on any condition. If calibrator was set back to 0-hour control, there was a significant effect for time-point ( $P < 0.01$ ) specifically from 0-hour to 3-days. The mean fold change for all conditions between 3- and 10-days was  $4.3 \pm 1.42$ . With CT 0-hour as calibration, this increased to  $40.1 \pm 13.3$ . These results indicate that for MHC7 there was a substantial and significant increase in gene expression from 0-hour to 3-days, which remained unchanged from 3- to 10-days and unaffected by testosterone treatment. At 3-days there is a trend for treatment having higher expression, which

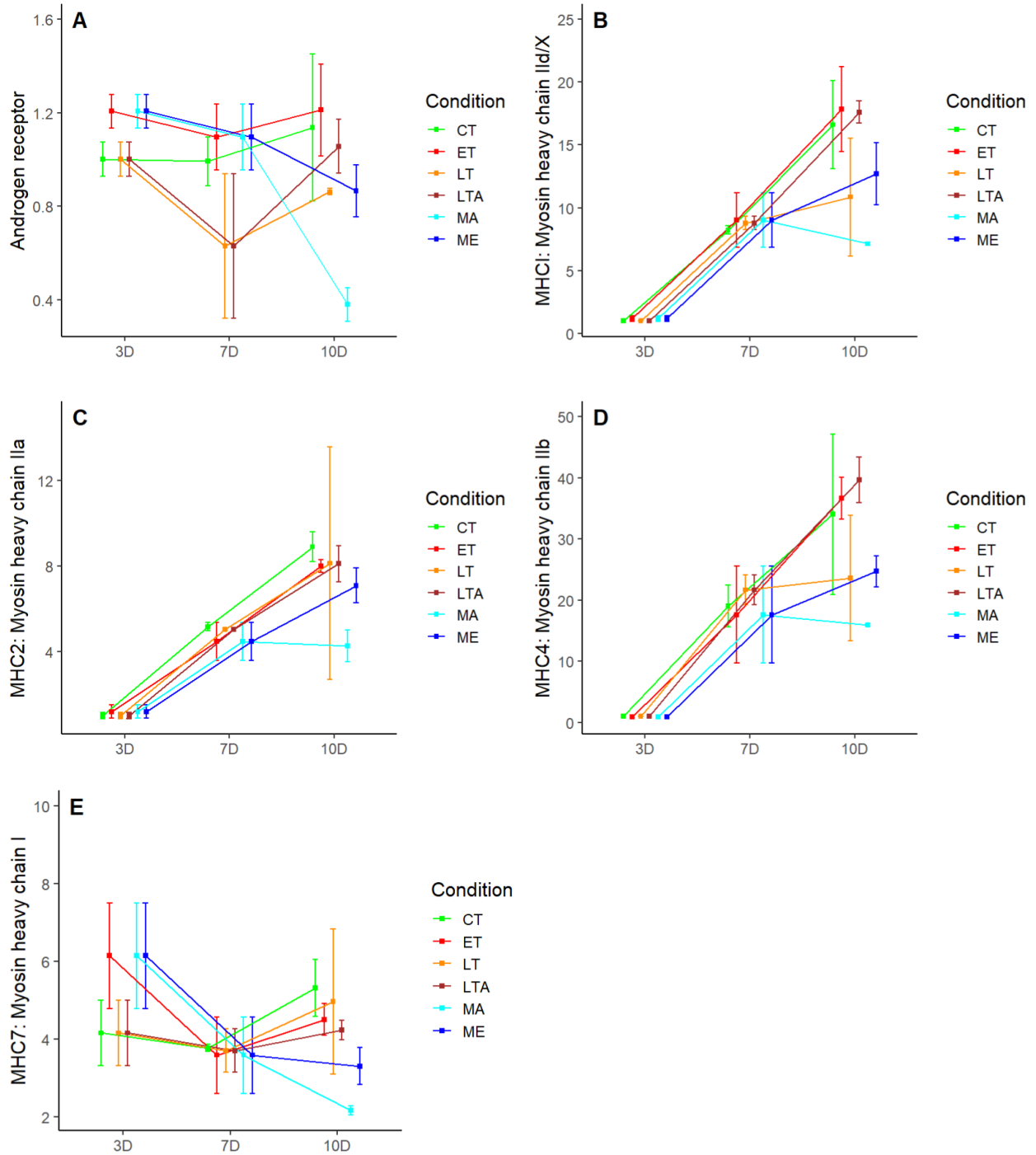
conversely, at 10-days trends toward less expression for memory compared with all other conditions. Mean fold change  $\pm$  SD is summarized in [table 8](#). and illustrated in figure 12.

**Table 9. MHC7 fold change summary**

condition	timepoint	Mean	SD	Min	Max	condition	timepoint	Mean	SD	Min	Max
CT	3D	4.16	1.20	3.31	5.01	LTA	3D	4.16	1.20	3.31	5.01
CT	7D	3.77	0.13	3.68	3.86	LTA	7D	3.71	0.79	3.15	4.27
CT	10D	5.32	1.04	4.59	6.06	LTA	10D	4.23	0.35	3.98	4.48
ET	3D	6.15	1.93	4.79	7.51	MA	3D	6.15	1.93	4.79	7.51
ET	7D	3.59	1.39	2.61	4.57	MA	7D	3.59	1.39	2.61	4.57
ET	10D	4.51	0.58	4.09	4.92	MA	10D	2.17	0.16	2.05	2.28
LT	3D	4.16	1.20	3.31	5.01	ME	3D	6.15	1.93	4.79	7.51
LT	7D	3.71	0.79	3.15	4.27	ME	7D	3.59	1.39	2.61	4.57
LT	10D	4.97	2.64	3.10	6.84	ME	10D	3.31	0.67	2.84	3.78



**Figure 12. MHC7:** Illustrating mean fold change  $\pm$  SE across time. Herein we observe a decrease in gene expression from 0-hour and to 3-days (not shown), from hence this trend turns flat for all conditions except MA and ME which continue with a negative directionality, albeit no change is significant.



**Figure 13. Combined plot of all genes with fold change  $\pm$  SE.** The only significant effects are for time. **A:** Illustrate the androgen receptor whereby the memory conditions (MA and ME) directionality moves non-significantly opposite to all other conditions from 7- to 10-days, MA – CT ( $P = 0.053$ ). **B:** MHC1, shows how the memory conditions trend toward less increase in gene expression compared with all other conditions. **C:** MHC2, illustrating how the MA condition alone trends toward less gene expression compared with the overall pattern. **D:** MHC4, illustrate the same trend for the memory conditions trending toward less gene expression compared with the other conditions. **E:** MHC7, once again illustrating the memory conditions trending toward a deviating from the overall pattern.

## 4.2.0 Discussion

The objective of this thesis was to investigate the potential role of testosterone in facilitating a memory response in SkM cells, comparable to that observed by resistance training alone. This was achieved by examining the effects of repeated testosterone treatments on the morphology and gene expression response in C2C12 cells. Due to significant delays in the initiation of the experiments, one technical replicate was lost, including the time to analyze important measures, such as epigenetic methylation and myonucleic abundance. As a result, the interpretation of the produced data is limited, and important questions remain unanswered. Nevertheless, the obtained data do lend insights and highlight areas of interest for future studies regardless of these limitations.

### 4.2.1 Main findings

The present study demonstrated a significant effect of both time and testosterone treatment on myotube diameter and area, whereby the treated cells were significantly larger compared to untreated control. Furthermore, the repeatedly treated MEM conditions exhibited significantly larger myotube diameter than the single treated LATE and ET conditions (figure 5). Moreover, myotube area was significantly affected by testosterone treatment, with all treated conditions exhibiting an acute increase to the next time-point superior to control. Interestingly, the ET condition grew significantly more than control from the 3- to 7-day time-points. However, this effect plateaued and resulted in the ET condition growing significantly less than control from the 7- to 10-day time-point, resulting in a non-significant difference in myotube area at 10-days. The LT condition exhibited greater myotube area growth from 7- to 10-days than control, ET, and LTA conditions. Additionally, the memory condition ME exhibited greater absolute myotube area, and myotube growth from 3- to 10-days compared with all other conditions. Moreover, the contrast analysis also revealed that the combined effects of ET and LT treated conditions were significantly less than the ME condition. Further supported by the magnitude of change from 7- to 10-days in the LT condition being significantly less than ME. Conversely, the MA memory condition, receiving a 4-hour acute testosterone dose at both 3 and 7 days, was not significantly different from either control, ET, or LTA conditions. Interestingly, MA grew significantly less than the LT condition from 7- to 10-days (figure 6A). Furthermore, these changes in myotube area were all abolished when removing the myoblast data, whereby the change from 7- to 10-days was either

non-significant or negatively significant for all treated conditions (see figure 6B). The individual analysis of the myobranche area fell in line with the observations of the myotube area. Whereby the ME condition exhibited significantly greater growth and myobranche area compared to all other conditions from 7- to 10-days. Interestingly, no significant effect of treatment on myotube number was observed, nor did this change over time, albeit showing a non-significant trend to increase over time. In the gene expression analysis, no overall significant differences were found between treated conditions and control. However, the memory conditions tended to non-significantly deviate from the other untreated or single-treated conditions. In the memory conditions, the AR gene expression from 7 to 10-days tended toward a decrease, and there was less pronounced increase in gene expression for the MHC I, 2, and 4 isoforms (Figure 13A-D). The MHC7 isoform deviated from the overall pattern via continuously decreasing from 7- to 10-days whereas all other conditions seemed to plateau (figure 13E). Overall, testosterone treatment had a notable impact on morphology, whereby the memory condition with the repeated treatment being left on for more than 4-hours proved advantageous in increasing myotube diameter, area, and myobranche area. Exhibiting synergistic effects in myotube area. No treatment had a significant effect on target gene expression, albeit exhibiting a non-significant tendency for an effect in gene expression for the memory conditions.

#### 4.2.2 The effects of testosterone treatment on C2C12 morphology

The current consensus in existing literature is that testosterone treatment, both *in-vivo* and *in-vitro*, augment SkM hypertrophy (Bhasin et al., 2001; Dubois et al., 2012; Herbst & Bhasin, 2004; Hughes, 2014; Sinha-hikim et al., 2004). Consistently showing that testosterone treatment augment cell hypertrophy characterized by increased myotube numbers and diameter compared to untreated controls (Deane et al., 2013; Hughes, 2014; Hughes et al., 2016; Wannenes et al., 2008). These are in line with the present study, whereby testosterone treatment exhibited a notable impact on cell morphology causing increased myotube diameter (figure 5). However, conversely, the present study demonstrated no significant increase in myotube numbers for neither treatment nor time, despite observing an upward trend in absolute values (figure 3). This is likely explained by the myobranches being counted as a single cell when they are likely multiple myotubes fused together. Interestingly, although no previous study have measured myotube area after testosterone

treatment, they have demonstrate increased myotube area after longer culture times (Niioka et al., 2018). Similarly, in the present study myotube area increased over time, which testosterone treatment significantly augmented for the ET condition from 3- to 7-days, for the LT condition from 7- to 10-days, and the ME condition from 3- to 10-days. Interestingly, the ET condition plateaued from 7- to 10-days resulting in ET no longer being larger than control at 10-days. Suggesting that the acute dose at day 3 washed out between day 7 and 10, and no longer proved advantageous for hypertrophy. However, upon repeated treatment with a chronic dose of testosterone (ME), the cells underwent augmented hypertrophy at a greater magnitude than the single chronic treatment (LT) during the same time span. This effect was also larger than the combined effects of ET and LT. Suggesting that the ME condition gained a synergistic effect of the repeated treatment. Conversely, the MA condition received an acute testosterone dose at the same time as ME, albeit did not gain the same benefits exhibiting no difference compared with either control or ET. This effect was also observed in the LTA condition, whereby the late acute dose did not prove advantageous compared with control (table 3A and figure 6A).

Interestingly, in this batch of C2C12 cells a remarkable level of proliferation and differentiation was observed, resulting in the formation of multiple structures consisting of fused and branching myotubes, termed "myobranched" (figure 4B). The presence of these myobranched introduced substantial variability to the dataset due to their size being magnitudes larger than all other myotubes. Moreover, these were considered a single myotube rather than multiple, likely limiting the myotube number measurements. They were also not eligible for myotube diameter measurements due to their heterogeneity in structure and would therefore pose a limitation to these measurements too. By excluding the myobranched data from the myotube area analysis, all the observed effects of testosterone from 7- to 10-days were abolished (figure 6B). The individual analysis of these myobranched found the ME condition to be nearly significantly larger than all other conditions (figure 7). This condition being exposed to testosterone for 4-hours at 3-days, and then again at 7-days with the testosterone media left until 10-days. Conversely, the MA condition, receiving testosterone for 4-hours at both timepoints was no different from the other treated conditions. Although limited by a small sample size, this suggests that the ME condition took significant benefits from the excess testosterone but that the single treated conditions, and repeated acute treatment of 4-hours in the MA condition did not pose additional benefits.

There has been one comparable study employing a memory of testosterone design, conducted on live rodents, which confirmed a memory effect characterized by increased hypertrophy in response to later exercise in previously testosterone versus placebo treated rodents (Egner et al., 2013). In their study, Egner and colleagues (2013) conducted a testosterone and exercise overload combination, and demonstrated myonuclear permanence, whereby the myonuclei gained because of testosterone treatment remained elevated compared to control despite removal of testosterone. Combined testosterone treatment with exercise overload, resulting in the observation of myonuclear permanence, where the elevated myonuclei gained due to testosterone treatment persisted despite its removal. Indeed, even after a 3-month period, which accounted for 12% of the mouse lifespan, the treated group had approximately twice the number of myonuclei compared to sham. Furthermore, when overload was introduced after this period, the previously treated group exhibited a 31% increase in SkM cross-sectional area within the first 6 days, while the sham group only showed a 6% increase. Thus, suggesting that the observed myonuclear permanence reflects a memory of previous testosterone exposure. In contrast, the present study focused on repeated testosterone treatment rather than incorporating an exercise stimulus. Interestingly, for myotube diameter, the repeated treatment of testosterone resulted in the memory conditions growing significantly larger than the late (LATE) and early treated (ET) conditions (figure 5). With the magnitude of change in MEM being larger than LATE albeit, and somewhat contradictory, no larger than the combined effects of ET and LATE. This contradiction limits the interpretation; however, the data nonetheless suggest that the repeated treatment proved additive if not synergistic for myotube diameter. Interestingly, the ET condition continued to grow in diameter throughout the experiment despite only an acute 4-hour exposure. Proposing the cells take advantage of the acute treatment of testosterone long after exposure. Similarly, testosterone treatment resulted in a significantly larger myotube area compared to control. Whereby the repeated treatment of the ME condition displayed a significantly larger hypertrophy compared with all other conditions (figure 6A). Indeed, the ME condition also exhibited a synergistic effect of the repeated treatment as observed by ME being superior to both the magnitude of change from 7- to 10-days in the single treated LT condition, and the combined effects of ET and LT across the same time span. Conversely, the MA condition did not exhibit this effect and was not different from control. Thereby suggesting that the memory effect relies on testosterone availability rather than the acute treatment. This is further supported in the myobranche analysis, whereby the ME condition

displayed a significantly larger area than control and late, with near-significance compared with ET ( $P = 0.055$ ) and MA ( $P = 0.08$ ). Suggesting that the repeated acute dose of testosterone did not elicit additional effects, but that a chronic treatment does. Overall, the data indicates that testosterone augments hypertrophy for myotube diameter and area when compared with untreated control. Moreover, exhibiting a contradictory effect for the early treated condition when comparing myotube diameter and area data. Whereby ET myotube diameter continued to grow throughout the experiment, whilst the myotube area plateaued by day 7, resulting in no difference from control at day 10. However, this contradiction could be a result of the measurement error as posed by the myobranched. The late treated conditions exhibited differing effects whereby the chronic availability of testosterone in LT proved superior and facilitated increased hypertrophy compared with control, ET and LTA. The availability of testosterone also seemed to drive the memory effect within the repeatedly treated conditions, whereby the ME condition exhibited clear evidence for a memory effect. Which was not observed in the MA condition. These results are indicative of the presence of a memory effect, however, they are also limited by the data displaying large variance, small sample size, and several measurement errors posed by the myobranched. Further limitations are mentioned in section 4.2.5.

### 4.2.3 The effects of testosterone treatment on C2C12 fold gene expression

Existing literature on testosterone treatment has reported dose-dependent effects on AR gene expression. Wannenes and colleagues (2008) treated C2C12 cells with 0.1, 1, and 10 nM testosterone post removal of serum. Herein they observed a dose-response increase in AR gene expression. Conversely, Hughes (2014) dosed their C2C12 cells with 50, 100, and 500nM at a similar time-point, whereby they observed no significant difference in AR gene expression levels across any conditions. Furthermore, AR gene expression decreases from proliferating myoblasts to formed myotubes in the C2C12 cell line (Hughes, 2014; Sheppard et al., 2011). Additionally, the C2C12 cells contain reportedly low levels of ARs, with proliferating cells containing 0.1% of the level of AR mRNA present in adult mouse gastrocnemius muscle (Altuwaijri et al., 2004; Y. Chen et al., 2008). These findings are consistent with the present study, whereby the AR gene expression dropped significantly from 0-hour (proliferating myoblasts) to 3-days (formed myotubes). Surprisingly, repeated testosterone treatment resulted in a further decrease in AR gene



expression from 7- to 10-days, suggesting that the cells saturated their AR content. Interestingly, despite the ME condition receiving higher objective dose of testosterone over time, the MA condition exhibited a greater decrease in AR expression. This suggests that the presence of testosterone in media might attenuate the decrease in AR expression [by counteracting some of the inhibitory effect,] despite the ARs being saturated. Overall, in the repeatedly treated conditions, testosterone non-significantly tended to decrease AR gene expression. The data, limited by the small sample size, did not provided clear evidence of a memory effect, thus limiting the interpretation of this mechanism. However, these results could also posit that for the C2C12 cell line, the traditional AR-mediated pathways are less pronounced and that the non-traditional or indirect pathways are prioritized to account for the lower levels of ARs.

The myosin heavy chains (MyHC) are markers of fibre type and terminal differentiation. In adult SkM three isoforms are present and separated by their functional properties: one slow twitch (MyHC I) and two fast twitch (MyHC IIa and IIx/d), with mice expressing a third fast twitch isoform (MyHC IIb); (Schiaffino & Reggiani, 1996). Resistance training is associated with a transition from MyHC IIx/d to the IIa isoform in SkM, which then undergo the most hypertrophy (Adams & Bamman, 2012; Plotkin et al., 2021). Studies have demonstrated that 50nM testosterone treatment in primary human SkM increase MyHC content, as measured by immunostaining (Serra et al., 2011). Wannenes and colleagues (2008) observed elevated mRNA levels of MHC7 (MyHC I), MHC1 (MyHC IIx/d), and MHC4 (MyHC IIb) isoforms in C2C12 cells treated with 10nM testosterone at the day of differentiation and remained significantly elevated at day 2 post treatment. This effect was most prominent in the MyHC I isoform. However, the difference between treated cells and control disappeared by day 4. Overall, these findings indicate that testosterone augments MyHC expression in the early stages of differentiation, but are leveled out comparable to control by day 4 post treatment. In the present study, however, treatment of testosterone was done further into the differentiated state at day 3. The effects measured herein are inconclusive due to the limitations in sample size, although tendencies are observed. For MyHC I, in line with other reports, the gene expression increased substantially when cells started differentiating. Interestingly, in the memory conditions, there was a trend of elevated expression at day 3, which decreased from day 3 to 10, deviating from the other conditions where expression remained unchanged from day 3 to 10. Surprisingly, this trend for the memory conditions deviating from the overall pattern of all other conditions was observed in the fast twitch MyHC isoforms as

well. Whereby, the memory conditions tended to have less pronounced of an increase in gene expression from day 7 to 10. Suggesting that the repeated dose of testosterone attenuated the increase in MyHC gene expression. The reason behind this effect leads into speculation, although there could be a shift in priorities in these cells with the repeated dose enabling other areas to augment hypertrophy, such as protein synthesis, ribosomal biogenesis, miRNAs, and sarcomere integrity (Wyce et al., 2010). The data was insufficient to determine the presence of a memory effect, thus preventing any definitive conclusions on this matter.

#### 4.2.4 C2C12 memory of previous testosterone treatment

The present study suggests the presence of a memory of previous testosterone treatment in C2C12 myotube diameter and area. Derived from observations of the ME condition exhibiting a synergistic hypertrophy upon second treatment. Interestingly, the hypertrophic effect is most prominent in conditions whereby testosterone is available for longer than 4-hours, as observed by the ME vs MA, and LT vs LTA results. Conversely, there is limited evidence of a memory effect from repeated testosterone treatment on C2C12 myotube numbers, and target gene expression. However, the gene expression analysis indicates that the AR is not affected by, or possibly negatively influenced by, the treatment of testosterone. Together with the evidence for C2C12 expressing less AR compared with live organisms. It is reasonable to hypothesize that the effect of repeated testosterone is facilitated by non-traditional androgenic mechanisms, whereby the availability of testosterone is increasingly important. However, the constraints posed by experiment limitations make it difficult to draw conclusive statements, emphasizing the need for additional data to derive insightful conclusions.

Speculatively, the generally low levels of ARs in C2C12 cell lines might pose a challenge to observe a translatable memory effect in humans, even in a larger sample. Testosterone's primary pathway of action is mediated by ARs (Dubois et al., 2012; Hughes et al., 2016). Given the constriction of this pathway, it may pose challenging to adequately stimulate the necessary mechanisms for a AR-mediated memory effect. Possibly making C2C12 cells an inadequate model for evaluating the AR-mediated memory of testosterone. Therefore, for future studies the use of human primary cells, or a substantially larger sample of C2C12 is ideal. A different approach

might also be more fruitful, such as including an exercise stimulus to investigate whether the early treatment facilitates increased hypertrophy to exercise compared with control.

Furthermore, the inclusion of the planned measurements of myonuclear abundance and epigenetic methylation would naturally strengthen the insights and provide specific gene targets for further analysis. These data could then be correlated with the genes identified by Wyce and colleagues (2010) to elucidate specific gene pathways involved in a possible memory mechanism.

#### 4.2.5 Limitations of this thesis

Unfortunately, this study faced major limitations due to persistent and random cell contamination, leading to substantial delays in experiment initiation. Cell contaminations are the most persistent problems arising in cell culture and pose a major challenge. Most contaminations are bacteria, fungi, and yeast (Niehues et al., 2020). Despite multiple attempts to isolate the source of contamination, the problem persisted without successful identification. Even with sterility protocols far exceeding standards, the contaminations returned at random. This problem resulted in several batches of cells being terminated and the need for complete sterilization of the laboratory. Despite purchase of completely new sets of culture medias, cleansing of laboratory equipment and stringent protocols, the problem persisted. The contaminants were not identified as mycoplasma or yeast but were consistent with typical bacterial presence. After discovering the article from Niehues (2020), which found both their tap and water purification systems to be contaminated with ethanol resistant bacteria. We suspected the water tap used to cleanse waste bins for media and disposable tips to contain contaminants with possible resistance to ethanol. These contaminants could, thus, be transferred from these equipment surfaces and contaminate culture flasks undeterred by ethanol spray. Moreover, the water bath used to warm solutions is provided with double distilled water from our own purification system, which, if contaminated, could leave small contaminants incubating in the warm environment of the bath increasing risk of bacterial infection in the cultures. Indeed, a study investigating the presence of bacteria in a typical water purification system observed several strains of bacteria at multiple stages of the system including the final supposedly pure stages. Highlighting the need for extra stringent service and testing of these systems (Penna et al., 2002). Indeed, upon inspecting the water tap used for cleaning, a mass of green algae-like substance was found inside the tap aerator. Algae is

consistently associated in a symbiotic type relationship with bacteria (Ramanan et al., 2016). The tap aerator was then submerged in Virkon (1%) for 48 hours and later rinsed. To the author's knowledge, the water distillery remained un-serviced. Therefore, any flask in the bath was treated as if it was carrying an infectant. The culture hood was therefore sectioned into 4 separate domains (waste, work, clean, tips and aliquots – from left to right) to limit what components of culture touched what surface. All components in contact with the water bath were aliquoted from their respective containers into appropriate and sterile falcons or flasks. Prior to the introduction of culture flasks or wells, water bath flasks were removed, and the surfaces of the hood were treated with both ethanol and Virkon. These precautions resulted in no recurring contamination and enabled the start of the experiment. Unfortunately, time lost is not regained, and we were unable to complete the third technical replicate and methylation measurements on time. Additionally, issues with the acquisition of a mounting chamber for the fixed cells to the microscope resulted in the myonucleic data also not being completed on time. The limitations significantly restrict the sample size and information gathered, consequently limiting the ability to derive meaningful conclusions regarding the research question. Additionally, considering the highly proliferative and differentiative nature of this batch of C2C12 cells, the author recommends conducting at least 4, if not more, replicates to adequately sample the myoblasts. In conclusion, when laboratory contaminations arise, and persist, it becomes increasingly important to question even the least likely of possibilities. Determining whether the water tap or water distillery was or is infected requires specific examination, which the author highly recommends the faculty to perform.

Another limitation is the generalizability of C2C12 cell culture into *in-vivo* conclusions. Moreover, 2D-culture is even less representative compared to 3D-culture which better mimic morphologies observed in living organisms. In addition, C2C12 cells may not be an optimal model for assessing a memory of testosterone due to their significantly lower abundance of ARs, with only 0.1% of the mRNA expression levels compared with adult mouse gastrocnemius muscle (Altuwaijri et al., 2004). In conclusion, to make an optimal investigation into the memory of testosterone mechanism, the author suggests using a combination of 2D and 3D C2C12, preferably in 4 or more replicates, including human primary SkM cells to fully elucidate on this mechanism.

### 4.3.0 Conclusions and future directions

This study investigated the effects of repeated treatment of testosterone in a C2C12 cell culture model. Herein observing testosterone to positively augment hypertrophy through increases in myotube diameter and area, whereby repeated treatment of testosterone with availability in media post 4-hours, resulted in synergistic hypertrophic effects compared with single treatment. Moreover, the repeated treatment of testosterone may lead to the saturation of the AR in C2C12 cells, as indicated by the trend for a decrease in AR mRNA levels. Interestingly, repeated treatment of testosterone also resulted in less pronounced of an increase in MyHC isoform mRNA expression levels. Suggesting that the repeated treatment shifted the cell priorities into other domains to augment its effects. However, this study found limited evidence, for the existence of a memory effect on target gene expression as all trends proposed were non-significant. However, this was contradicted by morphological data whereby repeated treatment presented with a memory effect on myotube diameter and area. Finally, this study was also severely limited by experiment constraints and lack of data. Thus, a clear conclusion on this mechanism is not within the reach of this dataset.

In conclusion, for an optimal investigation of the testosterone memory mechanism, it is recommended to utilize a combination of 2D and 3D C2C12 cultures, preferably with four or more replicates. Additionally, including human primary SkM would provide further insight into this mechanism in a model organism sharing a human phenotype. Using exercise stimulus would also elucidate whether testosterone has other memory mechanisms. With these models, measuring myonuclei enables insight into the myonuclear permanence hypothesis. In addition, measurement of epigenetic methylation would open a vast domain of target genes for further analysis which may elucidate on what mechanisms are prioritized with the repeated treatment of testosterone, and whether the memory mechanism is present because of this androgenic hormone.

## V. List of figures

Figure 1: Illustrating the hypothalamus-pituitary-gonadal axis. ....	4
<b>Figure 2:</b> Study design schematic indicating all time-points, isolations, treatments, and conditions.....	19
<b>Figure 3</b> Illustrating myotube numbers over time $\pm$ SEI. ....	28
<b>Figure 4</b> Representative example-images used in the morphological analysis. ....	31
<b>Figure 5.</b> Illustrate the change in mean Myotube Diameter ( $\mu m$ ) over time $\pm$ SE. ....	32
<b>Figure 6.</b> Mean change in Myotube Area ( $\mu m^2$ ) over time for all conditions $\pm$ SE.. ....	36
<b>Figure 7.</b> Mean myobranh area analysis andime for all conditions $\pm$ SE.. ....	36
<b>Figure 8. AR:</b> Illustrating the mean fold change $\pm$ SE across time. ....	38
<b>Figure 9. MHC1:</b> Illustrating the mean fold change $\pm$ SE across time. ....	40
<b>Figure 10. MHC2:</b> Illustrating the mean fold change $\pm$ SE across time.. ....	41
<b>Figure 11. MHC4:</b> Illustrate the mean fold change $\pm$ SE over time.. ....	43
<b>Figure 12. MHC7:</b> Illustrating mean fold change $\pm$ SE across time. ....	44
<b>Figure 13. Combined plot of all genes with fold change <math>\pm</math> SE. .</b> ....	45

## VI. References

- Adams, G. R., & Bamman, M. M. (2012). Characterization and regulation of mechanical loading-induced compensatory muscle hypertrophy. *Comprehensive Physiology*, 2(4), 2829–2870. <https://doi.org/10.1002/cphy.c110066>
- Alberts, B., Johnson, A., Lewis, J., Morgan, D., Raff, M., Roberts, K., & Walter, P. (2015). The molecular biology of the cell. In *Garland Science* (6th ed.). Taylor & Francis. [https://doi.org/10.1016/0014-5793\(86\)80238-1](https://doi.org/10.1016/0014-5793(86)80238-1)
- Allen, D. D., Caviedes, R., Cárdenas, A. M., Shimahara, T., Segura-Aguilar, J., & Caviedes, P. A. (2005). Cell lines as in vitro models for drug screening and toxicity studies. *Drug Development and Industrial Pharmacy*, 31(8), 757–768. <https://doi.org/10.1080/03639040500216246>
- Almeida, C. F., Fernandes, S. A., Ribeiro Junior, A. F., Keith Okamoto, O., & Vainzof, M. (2016). Muscle satellite cells: Exploring the basic biology to rule them. *Stem Cells International*, 2016. <https://doi.org/10.1155/2016/1078686>
- Altuwajri, S., Lee, D. K., Chuang, K., Ting, H., Yang, Z., Xu, Q., Tsai, M., Yeh, S., Hanchett, L. A., & Chang, H. (2004). of Skeletal Muscle – Specific Proteins and Muscle Cell Types. *October*, 25(1), 27–32.
- Anderson, E., & Durstine, J. L. (2019). Physical activity, exercise, and chronic diseases: A brief review. *Sports Medicine and Health Science*, 1(1), 3–10. <https://doi.org/10.1016/j.smhs.2019.08.006>
- Barone, B., Napolitano, L., Abate, M., Cirillo, L., Reccia, P., Passaro, F., Turco, C., Morra, S., Mastrangelo, F., Scarpato, A., Amicuzi, U., Morgera, V., Romano, L., Calace, F. P., Pandolfo, S. D., De Luca, L., Aveta, A., Sicignano, E., Trivellato, M., ... Crocetto, F. (2022). The Role of Testosterone in the Elderly: What Do We Know? *International Journal of Molecular Sciences*, 23(7), 1–21. <https://doi.org/10.3390/ijms23073535>
- Barrés, R., Yan, J., Egan, B., Treebak, J. T., Rasmussen, M., Fritz, T., Caidahl, K., Krook, A., Gorman, D. J. O., & Zierath, J. R. (2012). Short Article Acute Exercise Remodels Promoter Methylation in Human Skeletal Muscle. *Cell Metabolism*, 405–411.

<https://doi.org/10.1016/j.cmet.2012.01.001>

- Basaria, S. (2013). Reproductive Aging in Men. *Endocrinology and Metabolism Clinics of North America*, 42(2), 255–270. <https://doi.org/10.1016/j.ecl.2013.02.012>
- Bassil, N., Alkaade, S., & Morley, J. E. (2009). The benefits and risks of testosterone replacement therapy: A review. *Therapeutics and Clinical Risk Management*, 5(1), 427–448. <https://doi.org/10.2147/tcrm.s3025>
- Beiter, T., Nieß, A. M., & Moser, D. (2020). Transcriptional memory in skeletal muscle. Don't forget (to) exercise. *Journal of Cellular Physiology*, 235(7–8), 5476–5489. <https://doi.org/10.1002/jcp.29535>
- Bennett, N. C., Gardiner, R. A., Hooper, J. D., Johnson, D. W., & Gobe, G. C. (2009). Molecular cell biology of androgen receptor signalling. *International Journal of Biochemistry and Cell Biology*, 42(6), 813–827. <https://doi.org/10.1016/j.biocel.2009.11.013>
- Bhasin, S., Storer, T. W., Berman, N., Callegari, C., Clevenger, B., Phillips, J., Bunell, T. J., Tricker, P., Shirazi, A., & Casaburi, R. (1996). The Effects of Supraphysiological Doses of Testosterone on Muscle Size and Strength in Normal Men. *The New England Journal of Medicine*, 335, 1–7.
- Bhasin, S., Woodhouse, L., Casaburi, R., Singh, A. B., Bhasin, D., Berman, N., Chen, X., Yarasheski, K. E., Magliano, L., Dzekov, C., Dzekov, J., Bross, R., Phillips, J., Sinha-Hikim, I., Shen, R., & Storer, T. W. (2001). Testosterone dose-response relationships in healthy young men. *American Journal of Physiology - Endocrinology and Metabolism*, 281(6 44-6), 1172–1181. <https://doi.org/10.1152/ajpendo.2001.281.6.e1172>
- Bhasin, S., Woodhouse, L., Casaburi, R., Singh, A. B., Mac, R. P., Lee, M., Yarasheski, K. E., Sinha-hikim, I., Dzekov, C., Dzekov, J., Magliano, L., & Storer, T. W. (2005). Older Men Are as Responsive as Young Men to the Anabolic Effects of Graded Doses of Testosterone. *The Journal of Endocrinology*, 90(2), 678–688. <https://doi.org/10.1210/jc.2004-1184>
- Bickel, C. S., Cross, J. M., & Bamman, M. M. (2011). Exercise dosing to retain resistance training adaptations in young and older adults. *Medicine and Science in Sports and Exercise*, 43(7), 1177–1187. <https://doi.org/10.1249/MSS.0b013e318207c15d>



- Blau, H. M., Pavlath, G. K., Hardeman Choy-Pik Chiu, E. C., Silberstein, L., Webster Steven C Miller, S. G., & Webster, C. (1985). Plasticity of the Differentiated State. *Science*, *230*, 815.
- Blocquiaux, S., Gorski, T., Van Roie, E., Ramaekers, M., Van Thienen, R., Nielens, H., Delecluse, C., De Bock, K., & Thomis, M. (2020). The effect of resistance training, detraining and retraining on muscle strength and power, myofibre size, satellite cells and myonuclei in older men. *Experimental Gerontology*, *133*(November 2019), 110860. <https://doi.org/10.1016/j.exger.2020.110860>
- Box, G. E., & Cox, D. R. (1982). An analysis of transformations revisited, rebutted. *Journal of the American Statistical Association*, *77*(377), 209–210. <https://doi.org/10.1080/01621459.1982.10477788>
- Braga, M., Bhasin, S., Jasuja, R., Pervin, S., & Singh, R. (2012). Testosterone inhibits transforming growth factor- $\beta$  signaling during myogenic differentiation and proliferation of mouse satellite cells: Potential role of follistatin in mediating testosterone action. *Molecular and Cellular Endocrinology*, *350*(1), 39–52. <https://doi.org/10.1016/j.mce.2011.11.019>
- Brown, D., Hikim, A. P. S., Kovacheva, E. L., & Sinha-hikim, I. (2009). Mouse model of testosterone-induced muscle fiber hypertrophy : involvement of p38 mitogen-activated protein kinase-mediated Notch signaling. *European Journal of Endocrinology*. <https://doi.org/10.1677/JOE-08-0476>
- Bruusgaard, J. C., Johansen, I. B., Egner, I. M., Rana, Z. A., & Gundersen, K. (2010). Myonuclei acquired by overload exercise precede hypertrophy and are not lost on detraining. *Proceedings of the National Academy of Sciences of the United States of America*, *107*(34), 15111–15116. <https://doi.org/10.1073/pnas.0913935107>
- Burd, N. A., Gorissen, S. H., & Loon, L. J. C. Van. (2013). Anabolic Resistance of Muscle Protein Synthesis with Aging. *Exercise and Sport Science Reviews*, *41*(3), 169–173.
- Burger, H. G. (2002). Androgen production in women. *Fertility and Sterility*, *77*(4), 4–6.
- Cardaci, T. D., Machek, S. B., Wilburn, D. T., Heileson, L., & Willoughby, D. S. (2020). Receptor – DNA Binding and Wnt /  $\beta$  -Catenin Signaling without Increases in Serum / Muscle Androgens or Androgen Receptor Content. *Nutrients*, *12*, 1–17.

- Chen, M. M., Zhao, Y. P., Zhao, Y., Deng, S. L., & Yu, K. (2021). Regulation of Myostatin on the Growth and Development of Skeletal Muscle. *Frontiers in Cell and Developmental Biology*, 9(December), 1–10. <https://doi.org/10.3389/fcell.2021.785712>
- Chen, W., Datzkiw, D., & Rudnicki, M. A. (2020). Satellite cells in ageing: Use it or lose it. *Open Biology*, 10(5), 1–11. <https://doi.org/10.1098/rsob.200048>
- Chen, Y., Lee, N. K. L., Zajac, J. D., & MacLean, H. E. (2008). Generation and analysis of an androgen-responsive myoblast cell line indicates that androgens regulate myotube protein accretion. *Journal of Endocrinological Investigation*, 31(10), 910–918. <https://doi.org/10.1007/BF03346441>
- Chen, Yue, Zajac, J. D., & MacLean, H. E. (2005). Androgen regulation of satellite cell function. *Journal of Endocrinology*, 186(1), 21–31. <https://doi.org/10.1677/joe.1.05976>
- Chouinard, S., Yueh, M., Tukey, R. H., Giton, F., Fiet, J., Pelletier, G., Barbier, O., & Alain, B. (2008). *Journal of Steroid Biochemistry and Molecular Biology Inactivation by UDP-glucuronosyltransferase enzymes : The end of androgen signaling* & 109, 247–253. <https://doi.org/10.1016/j.jsbmb.2008.03.016>
- Claessens, F., Denayer, S., Van Tilborgh, N., Kerkhofs, S., Helsen, C., & Haelens, A. (2008). Diverse roles of androgen receptor (AR) domains in AR-mediated signaling. *Nuclear Receptor Signaling*, 6. <https://doi.org/10.1621/nrs.06008>
- Cooke, P. S., Nanjappa, X. M. K., Ko, C., Prins, G. S., & Hess, R. A. (2017). Estrogens in male physiology. *American Physiological Society*, 97, 995–1043. <https://doi.org/10.1152/physrev.00018.2016>
- Corona, G., Giagulli, V. A., Maseroli, E., Vignozzi, L., Aversa, A., Zitzmann, M., Saad, F., Mannucci, E., & Maggi, M. (2016). Testosterone supplementation and body composition: Results from a meta-analysis study. *European Journal of Endocrinology*, 174(3), R99–R116. <https://doi.org/10.1530/EJE-15-0262>
- Correa, C. S., Cunha, G., Marques, N., Oliveira-Reischak, Ã., & Pinto, R. (2016). Effects of strength training, detraining and retraining in muscle strength, hypertrophy and functional tasks in older female adults. *Clinical Physiology and Functional Imaging*, 36(4), 306–310.

<https://doi.org/10.1111/cpf.12230>

- Deane, C. S., Hughes, D. C., Sculthorpe, N., Lewis, M. P., Stewart, C. E., & Sharples, A. P. (2013). Impaired hypertrophy in myoblasts is improved with testosterone administration. *Journal of Steroid Biochemistry and Molecular Biology*, *138*, 152–161. <https://doi.org/10.1016/j.jsbmb.2013.05.005>
- Deichmann, U. (2016). *Epigenetics : The origins and evolution of a fashionable topic*. *416*, 249–254. <https://doi.org/10.1016/j.ydbio.2016.06.005>
- Demšar, J. (2006). Statistical comparisons of classifiers over multiple data sets. *Journal of Machine Learning Research*, *7*, 1–30.
- Deschenes, M., & Kraemer, W. J. (2002). Performance and Physiologic. *American Journal of Physical Medicine & Rehabilitation*, *November*, 3–16. <https://doi.org/10.1097/01.PHM.0000029722.06777.E9>
- Dubois, V., Laurent, M., Boonen, S., Vanderschueren, D., & Claessens, F. (2012). Androgens and skeletal muscle : cellular and molecular action mechanisms underlying the anabolic actions. *Cellular and Molecular Life Sciences*, 1651–1667. <https://doi.org/10.1007/s00018-011-0883-3>
- Egan, B., & Sharples, A. P. (2023). Molecular Responses to Acute Exercise and Their Relevance for Adaptations in Skeletal Muscle to Exercise Training. *Physiological Reviews*. <https://doi.org/10.1152/physrev.00054.2021>
- Egan, B., & Zierath, J. R. (2013). Exercise metabolism and the molecular regulation of skeletal muscle adaptation. *Cell Metabolism*, *17*(2), 162–184. <https://doi.org/10.1016/j.cmet.2012.12.012>
- Egner, I. M., Bruusgaard, J. C., Eftestøl, E., & Gundersen, K. (2013). A cellular memory mechanism aids overload hypertrophy in muscle long after an episodic exposure to anabolic steroids. *Journal of Physiology*, *591*(24), 6221–6230. <https://doi.org/10.1113/jphysiol.2013.264457>
- Eriksson, A. (2006). *STRENGTH TRAINING AND ANABOLIC STEROIDS: A comparative study of teh vastus lateralis, a thigh muscle and the trapezius, a shoulder muscle, of strengt-*

*trained athletes* (Issue 1032). Umeå University.

Estrada, M., Espinosa, A., Müller, M., & Jaimovich, E. (2003). Testosterone stimulates intracellular calcium release and mitogen-activated protein kinases via a G protein-coupled receptor in skeletal muscle cells. *Endocrinology*, *144*(8), 3586–3597.  
<https://doi.org/10.1210/en.2002-0164>

Evans, R. M. (1988). The Steroid and Thyroid Hormone Receptor Superfamily. *Science*, *240*(4854).

Feng, C., Wang, H., Lu, N., & Tu, X. M. (2013). Log transformation: Application and interpretation in biomedical research. *Statistics in Medicine*, *32*(2), 230–239.  
<https://doi.org/10.1002/sim.5486>

Ferey, J. L. A., Brault, J. J., Smith, C. A. S., & Witczak, C. A. (2014). Constitutive activation of CaMKK $\alpha$  signaling is sufficient but not necessary for mTORC1 activation and growth in mouse skeletal muscle. *American Journal of Physiology - Endocrinology and Metabolism*, *307*(8), E686–E694. <https://doi.org/10.1152/ajpendo.00322.2014>

Ferrando, A. A., Sheffield-Moore, M., Yeckel, C. W., Gilkison, C., Jiang, J., Achacosa, A., Lieberman, S. A., Tipton, K., Wolfe, R. R., & Urban, R. J. (2002). Testosterone administration to older men improves muscle function: Molecular and physiological mechanisms. *American Journal of Physiology - Endocrinology and Metabolism*, *282*(3 45-3), 601–607. <https://doi.org/10.1152/ajpendo.00362.2001>

Ferrando, A. A., Tipton, K. D., Doyle, D., Phillips, S. M., Cortiella, J., & Wolfe, R. R. (1998). Testosterone injection stimulates net protein synthesis but not tissue amino acid transport. *American Journal of Physiology - Endocrinology and Metabolism*, *275*(5 38-5), 864–871.  
<https://doi.org/10.1152/ajpendo.1998.275.5.e864>

Foradori, C. D., Weiser, M. J., & Handa, R. J. (2008). Non-genomic actions of androgens. *Frontiers in Neuroendocrinology*, *29*(2), 169–181.  
<https://doi.org/10.1016/j.yfrne.2007.10.005>

Forbes, G. B. (1985). The Dose Response Curve. *Metabolism*, *34*(6), 571–573.

Gardiner-Garden, M., & Frommer, M. (1987). CpG Islands in Vertebrate Genomes. *Journal of*

*Molecular Biology*, 196, 261–282.

Gayon, J. (2016). From Mendel to epigenetics : History of genetics De Mendel a. *Comptes Rendus - Biologies*, 339(7–8), 225–230. <https://doi.org/10.1016/j.crvi.2016.05.009>

Gibney, E. R., & Nolan, C. M. (2010). Epigenetics and gene expression. *Heredity*, 4–13. <https://doi.org/10.1038/hdy.2010.54>

Gorski, P. P., Tumer, D. C., Morton, J. P., Sharples, A. P., & Areta, J. L. (2023). Human skeletal muscle methylome after low carbohydrate energy balanced exercise. *BioRxiv*, March. <https://doi.org/10.1152/ajpendo.00029.2023>

Grech, A., Breck, J., & Heidelbaugh, J. (2014). Adverse effects of testosterone replacement therapy: An update on the evidence and controversy. *Therapeutic Advances in Drug Safety*, 5(5), 190–200. <https://doi.org/10.1177/2042098614548680>

Griggs, R. C., Kingston, W., Jozefowicz, R. F., Herr, B. E., Forbes, G., & Halliday, D. (1989). Effect of testosterone on muscle mass and muscle protein synthesis. *Journal of Applied Physiology*, 66(1), 498–503. <https://doi.org/10.1152/jappl.1989.66.1.498>

Grounds, M. D., White, J. D., Rosenthal, N., & Bogoyevitch, M. A. (2002). The Role of Stem Cells in Skeletal and Cardiac Muscle Repair. *Journal of Histochemistry & Cytochemistry*, 50(5), 589–610.

Gundersen, K. (2016). Muscle memory and a new cellular model for muscle atrophy and hypertrophy. *Journal of Experimental Biology*, 219(2), 235–242. <https://doi.org/10.1242/jeb.124495>

Hamilton, B. R., Lima, G., Barrett, J., Seal, L., Kolliari-Turner, A., Wang, G., Karanikolou, A., Bigard, X., Löllgen, H., Zupet, P., Ionescu, A., Debruyne, A., Jones, N., Vonbank, K., Fagnani, F., Fossati, C., Casasco, M., Constantinou, D., Wolfarth, B., ... Pitsiladis, Y. P. (2021). Integrating Transwomen and Female Athletes with Differences of Sex Development (DSD) into Elite Competition: The FIMS 2021 Consensus Statement. *Sports Medicine*, 51(7), 1401–1415. <https://doi.org/10.1007/s40279-021-01451-8>

Haren, M. T., Siddiqui, A. M., Armbrecht, H. J., Kevorkian, R. T., Kim, M. J., Haas, M. J., Mazza, A., Kumar, V. B., Green, M., Banks, W. A., & Morley, J. E. (2011). Testosterone

- modulates gene expression pathways regulating nutrient accumulation, glucose metabolism and protein turnover in mouse skeletal muscle. *International Journal of Andrology*, 34(1), 55–68. <https://doi.org/10.1111/j.1365-2605.2010.01061.x>
- Henwood, T. R., & Taaffe, D. R. (2008). *Detraining and Retraining in Older Adults Following Long-Term Muscle Power or Muscle Strength*. 63(7), 751–758.
- Herbst, K. L., & Bhasin, S. (2004). Testosterone action on skeletal muscle. *Current Opinion in Clinical Nutrition and Metabolic Care*, 7(3), 271–277. <https://doi.org/10.1097/00075197-200405000-00006>
- Hirsch, C., & Schildknecht, S. (2019). In vitro research reproducibility: Keeping up high standards. *Frontiers in Pharmacology*, 10(December), 1–9. <https://doi.org/10.3389/fphar.2019.01484>
- Hoberman, J. M., & Yesalis, C. E. (1995). The History of Synthetic Testosterone. *Scientific American*, February, 76–81.
- Hon, O. De, & Kuipers, H. (2015). *Prevalence of Doping Use in Elite Sports : A Review of Numbers and Methods*. 57–69. <https://doi.org/10.1007/s40279-014-0247-x>
- Hughes, D. C. (2014). *Mechanisms of androgen-induced hypertrophy: Lessons from muscle cell models*.
- Hughes, D. C., Stewart, C. E., Sculthorpe, N., Dugdale, H. F., Yousefian, F., Lewis, M. P., & Sharples, A. P. (2016). Testosterone enables growth and hypertrophy in fusion impaired myoblasts that display myotube atrophy: deciphering the role of androgen and IGF-I receptors. *Biogerontology*, 17(3), 619–639. <https://doi.org/10.1007/s10522-015-9621-9>
- Illingworth, R., Kerr, A., Desousa, D., Helle, J., Ellis, P., Stalker, J., Jackson, D., Clee, C., Plumb, R., Rogers, J., Humphray, S., Cox, T., Langford, C., & Bird, A. (2008). *A Novel CpG Island Set Identifies Tissue-Specific Methylation at Developmental Gene Loci*. 6(1). <https://doi.org/10.1371/journal.pbio.0060022>
- Ishimaru, T., Edmiston, W. A., Pages, L., & Horton, R. (1978). Splanchnic extraction and conversion of testosterone and dihydrotestosterone in man. *Journal of Clinical Endocrinology and Metabolism*, 46(4), 528–533. <https://doi.org/10.1210/jcem-46-4-528>

- Ivey, F. M., Tracy, B. L., Lemmer, J. T., Nissaiver, M., Metter, E. J., Fozard, J. L., & Hurley, B. F. (2000). *Effects of Strength Training and Detraining on Muscle Quality : Age and Gender Comparisons*. *55*(3), 152–157.
- Jones, M. E. E., Boon, W. C., Proietto, J., & Simpson, E. R. (2006). *Of mice and men : the evolving phenotype of aromatase deficiency*. *17*(2).  
<https://doi.org/10.1016/j.tem.2006.01.004>
- Juan-Manuel, A., Shoenfeld, Y., Rojas-Villarrage, A., Levy, R., Cervera, R. T., & Marincola M., F. (2013). Autoimmunity: From Bench to Bedside. In *Cancer and Autoimmunity*.  
<https://doi.org/10.1016/b978-0-444-50331-2.x5000-0>
- Kanayama, G., Jr, H. G. P., & D, M. (2018). Molecular and Cellular Endocrinology History and epidemiology of anabolic androgens in athletes and non- athletes. *Molecular and Cellular Endocrinology*, *464*, 4–13. <https://doi.org/10.1016/j.mce.2017.02.039>
- Kangaspeka, S., Stride, B., Métivier, R., Polycarpou-schwarz, M., Ibberson, D., Carmouche, R. P., Benes, V., Gannon, F., & Reid, G. (2008). Transient cyclical methylation of promoter DNA. *Nature*, *452*(March), 1–5. <https://doi.org/10.1038/nature06640>
- Kohl, M. (2015). *Introduction to Statistical Data Analysis with R*.
- Langhans, S. A. (2018). Three-dimensional in vitro cell culture models in drug discovery and drug repositioning. *Frontiers in Pharmacology*, *9*(JAN), 1–14.  
<https://doi.org/10.3389/fphar.2018.00006>
- Langley, B., Thomas, M., Bishop, A., Sharma, M., Gilmour, S., & Kambadur, R. (2002). Myostatin Inhibits Myoblast Differentiation by Down-regulating MyoD Expression \*. *Journal of Biological Chemistry*, *277*(51), 49831–49840.  
<https://doi.org/10.1074/jbc.M204291200>
- Li, G. W., Burkhardt, D., Gross, C., & Weissman, J. S. (2014). Quantifying absolute protein synthesis rates reveals principles underlying allocation of cellular resources. *Cell*, *157*(3), 624–635. <https://doi.org/10.1016/j.cell.2014.02.033>
- Lima, G., Kolliari-turner, A., Wang, G., Ho, P., Meehan, L., Roeszler, K., Seto, J., Malinsky, F. R., Karanikolou, A., Eichhorn, G., Tanisawa, K., Ospina-betancurt, J., Hamilton, B., Kumi,

- P. Y. O., Shurlock, J., Skiadas, V., Sem, P., Twycross-lewis, R., Kilduff, L., ... Borrione, P. (2022). The MMAAS Project : An Observational Human Study Investigating the Effect of Anabolic Androgenic Steroid Use on Gene Expression and the Molecular Mechanism of Muscle Memory. *Clinical Journal of Sports Medicine*, 00.
- Livak, K. J., & Schmittgen, T. D. (2001). Analysis of relative gene expression data using real-time quantitative PCR and the 2- $\Delta\Delta$ CT method. *Methods*, 25(4), 402–408.  
<https://doi.org/10.1006/meth.2001.1262>
- Ljungqvist, A. (2012). Half a century of challenges “. *Bioanalysis*, 4, 1531–1533.
- Maasar, M. F., Turner, D. C., Gorski, P. P., Seaborne, R. A., Strauss, J. A., Shepherd, S. O., Cocks, M., Pillon, N. J., Zierath, J. R., Hulton, A. T., Drust, B., & Sharples, A. P. (2021). The Comparative Methylome and Transcriptome After Change of Direction Compared to Straight Line Running Exercise in Human Skeletal Muscle. *Frontiers in Physiology*, 12(February), 1–17. <https://doi.org/10.3389/fphys.2021.619447>
- Mcfarlane, C., Plummer, E., Thomas, M., Hennebry, A., Ashby, M., Ling, N., Smith, H., Sharma, M., & Kambadur, R. (2006). *Myostatin Induces Cachexia by Activating the Ubiquitin Proteolytic System Through an NF- $\kappa$ B-Independent , FoxO1-Dependent Mechanism*. 514(June), 501–514. <https://doi.org/10.1002/jcp>
- Mendler, L., Baka, Z., Kovács-Simon, A., & Dux, L. (2007). Androgens negatively regulate myostatin expression in an androgen-dependent skeletal muscle. *Biochemical and Biophysical Research Communications*, 361(1), 237–242.  
<https://doi.org/10.1016/j.bbrc.2007.07.023>
- Miller, W. L., & Auchus, R. J. (2011). The Molecular Biology , Biochemistry , and Physiology of Human Steroidogenesis and Its Disorders. *Endocrine Reviews*, 32(February), 81–151.  
<https://doi.org/10.1210/er.2010-0013>
- Nelson, P. S., Clegg, N., Arnold, H., Ferguson, C., Bonham, M., White, J., Hood, L., & Lin, B. (2002). The program of androgen-responsive genes in neoplastic prostate epithelium. *Proceedings of the National Academy of Sciences of the United States of America*, 99(18), 11890–11895. <https://doi.org/10.1073/pnas.182376299>



- Ng, R. K., & Gurdon, J. B. (2008). Epigenetic inheritance of cell differentiation status. *Cell Cycle*, 7. <https://doi.org/10.4161/cc.7.9.5791>
- Niehues, H., Jansen, P. A. M., Rodijk-Olthuis, D., Rikken, G., Smits, J. P. H., Schalkwijk, J., Zeeuwen, P. L. J. M., & van den Bogaard, E. H. J. (2020). Know your enemy: Unexpected, pervasive and persistent viral and bacterial contamination of primary cell cultures. *Experimental Dermatology*, 29(7), 672–676. <https://doi.org/10.1111/exd.14126>
- Niioka, H., Asatani, S., Yoshimura, A., Ohigashi, H., Tagawa, S., & Miyake, J. (2018). Classification of C2C12 cells at differentiation by convolutional neural network of deep learning using phase contrast images. *Human Cell*, 31(1), 87–93. <https://doi.org/10.1007/s13577-017-0191-9>
- Ntanasis-Stathopoulos, J., Tzanninis, J. G., Philippou, A., & Koutsilieris, M. (2013). Epigenetic regulation on gene expression induced by physical exercise. *Journal of Musculoskeletal Neuronal Interactions*, 13(2), 133–146.
- Nussey, S. S., & Whitehead, S. A. (2001). *Endocrinology: An Integrated Approach*. BIOS Scientific Publishers Limited.
- Penna, V. T. C., Martins, S. A. M., & Priscila, G. M. (2002). Identification of bacteria in drinking and purified water during the monitoring of a typical water purification system. *BMC Public Health*, 11, 1–11.
- Pereira, D. G., Afonso, A., & Medeiros, F. M. (2015). Overview of Friedmans Test and Post-hoc Analysis. *Communications in Statistics: Simulation and Computation*, 44(10), 2636–2653. <https://doi.org/10.1080/03610918.2014.931971>
- Plotkin, D. L., Roberts, M. D., Haun, C. T., & Schoenfeld, B. J. (2021). Muscle fiber type transitions with exercise training: Shifting perspectives. *Sports*, 9(9), 1–11. <https://doi.org/10.3390/SPORTS9090127>
- Prescott, J., & Coetzee, G. A. (2006). *Molecular chaperones throughout the life cycle of the androgen receptor* \*. 231, 12–19. <https://doi.org/10.1016/j.canlet.2004.12.037>
- Psilander, N., Eftestøl, E., Cumming, K. T., Juvkam, I., Ekblom, M. M., Sunding, K., Wernbom, M., Holmberg, H. C., Ekblom, B., Bruusgaard, J. C., Raastad, T., & Gundersen, K. (2019).

- Effects of training, detraining, and retraining on strength, hypertrophy, and myonuclear number in human skeletal muscle. *Journal of Applied Physiology*, 126(6), 1636–1645.  
<https://doi.org/10.1152/jappphysiol.00917.2018>
- Ramanan, R., Kim, B. H., Cho, D. H., Oh, H. M., & Kim, H. S. (2016). Algae-bacteria interactions: Evolution, ecology and emerging applications. *Biotechnology Advances*, 34(1), 14–29. <https://doi.org/10.1016/j.biotechadv.2015.12.003>
- Ramaswamy, S., & Weinbauer, G. F. (2014). Endocrine control of spermatogenesis : Role of FSH and LH / testosterone. *Spermatogenesis*, 4(March), 37–41.  
<https://doi.org/10.1080/21565562.2014.996025>
- Riba, A., Nanni, N. Di, Mittal, N., Arhné, E., Schmidt, A., & Zavolan, M. (2019). Protein synthesis rates and ribosome occupancies reveal determinants of translation elongation rates. *Proceedings of the National Academy of Sciences of the United States of America*, 116(30), 15023–15032. <https://doi.org/10.1073/pnas.1817299116>
- Rodriguez, J., Vernus, B., Toubiana, M., Jublanc, E., Tintignac, L., Leibovitch, S., & Bonniou, A. (2011). Myostatin inactivation increases myotube size through regulation of translational initiation machinery. *Journal of Cellular Biochemistry*, 112(12), 3531–3542.  
<https://doi.org/10.1002/jcb.23280>
- Roselli, C. F. (2007). *Brain aromatase : Roles in reproduction and neuroprotection* & 106, 143–150. <https://doi.org/10.1016/j.jsbmb.2007.05.014>
- Russel, N., & Grossmann, M. (2019). Estradiol as a male hormone. *European Journal of Endocrinology*.
- Sailani, M. R., Halling, J. F., Møller, H. D., Lee, H., Plomgaard, P., Pilegaard, H., Snyder, M. P., & Regenberg, B. (2019). Lifelong physical activity is associated with promoter hypomethylation of genes involved in metabolism , myogenesis , contractile properties and oxidative stress resistance in aged human skeletal muscle. *Scientific Reports*, 9, 1–11.  
<https://doi.org/10.1038/s41598-018-37895-8>
- Schiaffino, S., & Reggiani, C. (1996). Molecular diversity of myofibrillar proteins: Gene regulation and functional significance. *Physiological Reviews*, 76(2), 371–423.

<https://doi.org/10.1152/physrev.1996.76.2.371>

Seaborne, R. A., Strauss, J., Cocks, M., Shepherd, S., O'Brien, T. D., Van Someren, K. A., Bell, P. G., Murgatroyd, C., Morton, J. P., Stewart, C. E., & Sharples, A. P. (2018). Human Skeletal Muscle Possesses an Epigenetic Memory of Hypertrophy. *Scientific Reports*, 8(1), 1–17. <https://doi.org/10.1038/s41598-018-20287-3>

Seiliez, I., Cédric, G., Taty, T., Bugeon, J., Dias, K., Sabin, N., & Gabillard, J. (2013). General and Comparative Endocrinology Myostatin induces atrophy of trout myotubes through inhibiting the TORC1 signaling and promoting Ubiquitin – Proteasome and Autophagy-Lysosome degradative pathways. *General and Comparative Endocrinology*, 186, 9–15. <https://doi.org/10.1016/j.ygcen.2013.02.008>

Serdar, C. C., Cihan, M., Yücel, D., & Serdar, M. A. (2021). Sample size, power and effect size revisited: Simplified and practical approach in pre-clinical, clinical and laboratory studies. *Biochemia Medica*, 31(1), 1–27. <https://doi.org/10.11613/BM.2021.010502>

Serra, C., Bhasin, S., Tangherlini, F., Barton, E. R., Ganno, M., Zhang, A., Shansky, J., Vandenberg, H. H., Travison, T. G., Jasuja, R., & Morris, C. (2011). The role of GH and IGF-I in mediating anabolic effects of testosterone on androgen-responsive muscle. *Endocrinology*, 152(1), 193–206. <https://doi.org/10.1210/en.2010-0802>

Sexton, C. L., Godwin, J. S., McIntosh, M. C., Ruple, B. A., Osburn, S. C., Hollingsworth, B. R., Kontos, N. J., Agostinelli, P. J., Kavazis, A. N., Ziegenfuss, T. N., Lopez, H. L., Smith, R., Young, K. C., Dwaraka, V. B., Frugé, A. D., Mobley, C. B., Sharples, A. P., & Roberts, M. D. (2023). Skeletal Muscle DNA Methylation and mRNA Responses to a Bout of Higher versus Lower Load Resistance Exercise in Previously Trained Men. *Cells*, 12(2). <https://doi.org/10.3390/cells12020263>

Sharples, A. P., Polydorou, I., Hughes, D. C., Owens, D. J., Hughes, T. M., & Stewart, C. E. (2016). Skeletal muscle cells possess a ‘memory’ of acute early life TNF- $\alpha$  exposure: role of epigenetic adaptation. *Biogerontology*, 17(3), 603–617. <https://doi.org/10.1007/s10522-015-9604-x>

Sharples, A. P., Stewart, C. E., & Seaborne, R. A. (2016). Does skeletal muscle have an ‘epi’-

- memory? The role of epigenetics in nutritional programming, metabolic disease, aging and exercise. *Aging Cell*, 15(4), 603–616. <https://doi.org/10.1111/accel.12486>
- Shen, L., Kondo, Y., Guo, Y., Zhang, J., Zhang, L., Ahmed, S., Shu, J., & Chen, X. (2007). Genome-Wide Profiling of DNA Methylation Reveals a Class of Normally Methylated CpG Island Promoters. *PLoS Genetics*, 3(10). <https://doi.org/10.1371/journal.pgen.0030181>
- Sheppard, R. L., Spangenburg, E. E., Chin, E. R., & Roth, S. M. (2011). Androgen receptor polyglutamine repeat length affects receptor activity and C2C12 cell development. *Physiological Genomics*, 43(20), 1135–1143. <https://doi.org/10.1152/physiolgenomics.00049.2011>
- Simpson, E. R. (2004). Aromatase: Biologic Relevance of Tissue-Specific Expression. *Seminars in Reproductive Medicine*, 22.
- Singh, R., Bhasin, S., Braga, M., Artaza, J. N., Pervin, S., Taylor, W. E., Krishnan, V., Sinha, S. K., Rajavashisth, T. B., & Jasuja, R. (2009). Regulation of myogenic differentiation by androgens: Cross talk between androgen receptor $\beta$ -catenin and follistatin/transforming Growth factor- $\beta$  signaling pathways. *Endocrinology*, 150(3), 1259–1268. <https://doi.org/10.1210/en.2008-0858>
- Sinha-Hikim, I., Artaza, J., Woodhouse, L., Gonzalez-Cadavid, N., Singh, A. B., Lee, M. I., Storer, T. W., Casaburi, R., Shen, R., & Bhasin, S. (2002). Testosterone-induced increase in muscle size in healthy young men is associated with muscle fiber hypertrophy. *American Journal of Physiology - Endocrinology and Metabolism*, 283(1 46-1), 154–164. <https://doi.org/10.1152/ajpendo.00502.2001>
- Sinha-hikim, I., Roth, S. M., Lee, M. I., Bhasin, S., Roth, S. M., Martin, I., & Testosterone-induced, S. B. (2003). Testosterone-induced muscle hypertrophy is associated with an increase in satellite cell number in healthy , young men. *American Journal of Physiology - Endocrinology and Metabolism*, 285, 197–205.
- Sinha-hikim, I., Taylor, W. E., Gonzalez-cadavid, N. F., Zheng, W. E. I., & Bhasin, S. (2004). *Androgen Receptor in Human Skeletal Muscle and Cultured Muscle Satellite Cells : Up-Regulation by*. 89(10), 5245–5255. <https://doi.org/10.1210/jc.2004-0084>

- Snijders, T., Leenders, M., Groot, L. C. P. G. M. De, Loon, L. J. C. Van, & Verdijk, L. B. (2019). Muscle mass and strength gains following 6 months of resistance type exercise training are only partly preserved within one year with autonomous exercise continuation in older adults. *Experimental Gerontology*, *121*(October 2018), 71–78.  
<https://doi.org/10.1016/j.exger.2019.04.002>
- Snijders, Tim, Aussieker, T., Holwerda, A., Parise, G., van Loon, L. J. C., & Verdijk, L. B. (2020). The concept of skeletal muscle memory: Evidence from animal and human studies. *Acta Physiologica*, *229*(3), 1–20. <https://doi.org/10.1111/apha.13465>
- Snyder, P. J., Peachey, H., Berlin, J. A., Hannoush, P., Haddad, G., Dlewati, A., Santanna, J., Loh, L., Lenrow, D. A., Holmes, J. H., Kapoor, S. C., Atkinson, L. E., Strom, B. L., & S, D. M. P. J. (2000). Hypogonadal Men \*. *Jcem*, *85*(8), 2670–2677.
- Stamatiades, G. A., & Kaiser, U. B. (2018). Gonadotropin regulation by pulsatile GnRH: Signaling and gene expression. *Molecular and Cellular Endocrinology*, *463*, 131–141.  
<https://doi.org/10.1016/j.mce.2017.10.015>
- Staron, R. S., Leonardi, M. J., Karapondo, L., Malicky, E. S., Falkel, J. E., Hagerman, F. C., & Hikida, R. S. (1991). Strength and skeletal muscle adaptations in heavy-resistance-trained women after detraining and retraining. *Journal of Applied Physiology*, *70*(2), 631–640.  
<https://doi.org/10.1152/jappl.1991.70.2.631>
- Taylor, W. E., Bhasin, S., Artaza, J., Byhower, F., Azam, M., Willard, D. H., Kull, F. C., Gonzalez-cadavid, N., Wayne, E., Bhasin, S., Artaza, J., Byhower, F., Azam, M., Willard, D. H., Kull, F. C., & Gonzalez-cadavid, N. (2001). Myostatin inhibits cell proliferation and protein synthesis in C 2 C 12 muscle cells. *American Journal of Physiology - Endocrinology and Metabolism*, *280*, 221–228.
- Thomas, M., Langley, B., Berry, C., Sharma, M., Kirk, S., Bass, J., & Kambadur, R. (2001). Myostatin , a Negative Regulator of Muscle Growth , Functions by Inhibiting Myoblast Proliferation \*. *Journal of Biological Chemistry*, *275*(51), 40235–40243.  
<https://doi.org/10.1074/jbc.M004356200>
- Trendelenburg, A. U., Meyer, A., Rohner, D., Boyle, J., Hatakeyama, S., Glass, D. J., Dj, G., &

- Torc, A. (2009). Myostatin reduces Akt / TORC1 / p70S6K signaling , inhibiting myoblast differentiation and myotube size. *American Journal of Physiology - Cell Physiology*, 296, 1258–1270. <https://doi.org/10.1152/ajpcell.00105.2009>.
- Tu, M. K., Levin, J. B., Hamilton, A. M., & Borodinsky, L. N. (2016). Calcium signaling in skeletal muscle development, maintenance and regeneration. *Cell Calcium*, 59, 11–54. <https://doi.org/10.1017/cbo9780511572937.003>
- Turner, D. C., Seaborne, R. A., & Sharples, A. P. (2019). Comparative Transcriptome and Methylome Analysis in Human Skeletal Muscle Anabolism , Hypertrophy and Epigenetic Memory. *Scientific Reports*, October 2018, 1–12. <https://doi.org/10.1038/s41598-019-40787-0>
- Venken, K., Gendt, K. De, Boonen, S., Ophoff, J., Bouillon, R., Swinnen, J. V, Verhoeven, G., & Vanderschueren, D. (2006). *Relative Impact of Androgen and Estrogen Receptor Activation in the Effects of Androgens on Trabecular and Cortical Bone in Growing Male Mice: A Study in the Androgen Receptor Knockout Mouse Model*. 21(4), 576–585. <https://doi.org/10.1359/JBMR.060103>
- Verhoeven, K. J., Vonholdt, B. M., & Sork, V. L. (2016). Epigenetics in ecology and evolution : what we know and what we need to know. *Molecular Ecology*, 25, 1631–1638. <https://doi.org/10.1111/mec.13617>
- WADA. (2021). *World Anti-Doping Code*.
- Wang, C., Swerdloff, R. S., Iranmanesh, A., Dobs, A., Snyder, P. J., Cunningham, G., Matsumoto, A. M., Weber, T., & Berman, N. (2000). Transdermal testosterone gel improves sexual function, mood, muscle strength, and body composition parameters in hypogonadal men. *Journal of Clinical Endocrinology and Metabolism*, 85(8), 2839–2853. <https://doi.org/10.1210/jc.85.8.2839>
- Wannenes, F., Caprio, M., Gatta, L., Fabbri, A., Bonini, S., & Moretti, C. (2008). Androgen receptor expression during C2C12 skeletal muscle cell line differentiation. *Molecular and Cellular Endocrinology*, 292(1–2), 11–19. <https://doi.org/10.1016/j.mce.2008.05.018>
- Wen, Y., Dungan, C. M., Mobley, C. B., Valentino, T., Walden, F. Von, & Murach, K. A.

- (2021). *Nucleus Type-Specific DNA Methylation Reveals Epigenetic “ Memory ” of Prior Adaptation in Skeletal Muscle*. 2(July), 1–11.
- West, R. M. (2022). Best practice in statistics: The use of log transformation. *Annals of Clinical Biochemistry*, 59(3), 162–165. <https://doi.org/10.1177/00045632211050531>
- Wilson, J. D. (2001). *Reproduction , Fertility and Development The role of 5  $\alpha$  -reduction in steroid hormone physiology*. 13.
- Wittert, G. A., Chapman, I. M., Haren, M. T., Mackintosh, S., Coates, P., & Morley, J. E. (2003). Oral testosterone supplementation increases muscle and decreases fat mass in healthy elderly males with low-normal gonadal status. *Journals of Gerontology - Series A Biological Sciences and Medical Sciences*, 58(7), 618–625. <https://doi.org/10.1093/gerona/58.7.m618>
- Wyce, A., Bai, Y., Nagpal, S., & Thompson, C. C. (2010). Research resource: The androgen receptor modulates expression of genes with critical roles in muscle development and function. *Molecular Endocrinology*, 24(8), 1665–1674. <https://doi.org/10.1210/me.2010-0138>
- Yaffe, D., & Saxel, O. (1977). Serial passaging and differentiation of myogenic cells isolated from dystrophic mouse muscle. *Nature*, 270.
- Yeo, I.-K., & Johnson, R. A. (2000). A new family of power transformations to improve normality or symmetry. *Biometrika*, 87(4), 954–959.
- Zhou, S. (2008). *Drugs Behave as Substrates , Inhibitors and Inducers of Human Cytochrome P450*. 310–322.
- Zuloaga, D. G., Puts, D. A., Jordan, C. L., & Breedlove, S. M. (2008). *The role of androgen receptors in the masculinization of brain and behavior : What we ’ ve learned from the testicular feminization mutation*. 53, 613–626. <https://doi.org/10.1016/j.yhbeh.2008.01.013>

## Appendix A

### Attestation of Authorship and the use of Artificial Intelligence

I formally announce that this submission is my personal work which, to the best of my knowledge, does not contain material previously generated by another person or artificial intelligence, unless specified.

Furthermore, I attest that the use of artificial intelligence (AI) within this thesis is solely in the purpose of a writers' assistance, whereby AI tools such as ChatGPT (OpenAI GPT-3.5, ChatGPT May 24 Version) have assisted the writing process by giving feedback and suggestions to improve language, clarity, conciseness, syntax, and order of information. AI has not been used for the purpose of gathering any information or sources, nor has any output been plagiarized. The primary prompt used for this purpose is:

“[example text]

Review this extract from my academic thesis as if you are a professor in the field of exercise science, physiology, and molecular biology. You are familiar with the terminology and so would the readers. Provide first with overall feedback on the language, syntax, clarity, and order of information. Provide with a bullet list whereby you take each individual sentence eligible for feedback as outlined and provide with suggestions for improvement”.

Moreover, AI has also been used as a coding assistant in RStudio. Herein no generalized prompt is used, rather, questions regarding the code syntax or structure, or regarding errors, and requests for lists of functions for specific packages with descriptions is prompted. In unison with traditional forums such as GitHub and Stack Overflow, including Kohl's "Introduction to Statistical Data Analysis with R" (Kohl, 2015), all code is carefully verified to be accurate and provide with the desired outcomes.

AI assistance in academia is a powerful tool, which when used correctly may enable increased efficiency and enhanced learning. However, it is important to acknowledge its limitations and never to use AI without careful scrutiny.